Published in final edited form as:
Acta Biomater. 2012 April ; 8(4): 1401–1421. doi:10.1016/j.actbio.2011.11.017.

Calcium phosphate ceramic systems in growth factor and drug delivery for bone tissue engineering: A review

Susmita Bose* and **Solaiman Tarafder**
W. M. Keck Biomedical Materials Research Laboratory, School of Mechanical and Materials Engineering, Washington State University, Pullman, WA 99164-2920, USA

Abstract

Calcium phosphates (CaPs) are the most widely used bone substitutes in bone tissue engineering due to their compositional similarities to bone mineral and excellent biocompatibility. In recent years, CaPs, especially hydroxyapatite and tricalcium phosphate, have attracted significant interest in simultaneous use as bone substitute and drug delivery vehicle, adding a new dimension to their application. CaPs are more biocompatible than many other ceramic and inorganic nanoparticles. Their biocompatibility and variable stoichiometry, thus surface charge density, functionality, and dissolution properties, make them suitable for both drug and growth factor delivery. CaP matrices and scaffolds have been reported to act as delivery vehicles for growth factors and drugs in bone tissue engineering. Local drug delivery in musculoskeletal disorder treatments can address some of the critical issues more effectively and efficiently than the systemic delivery. CaPs are used as coatings on metallic implants, CaP cements, and custom designed scaffolds to treat musculoskeletal disorders. This review highlights some of the current drug and growth factor delivery approaches and critical issues using CaP particles, coatings, cements, and scaffolds towards orthopedic and dental applications.

Keywords

Calcium phosphate nanoparticles; Coatings; Scaffolds; Cements; *In vitro* and *in vivo* studies

1. Introduction

Musculoskeletal diseases or disorders such as arthritis, osteoporosis, osteonecrosis, bone fracture, bone tumor, trauma due to sports, war and/or road traffic injuries, back pain and other spinal disorders cost society over $250 billion annually in the USA, and affects hundreds of millions of people across the world. It is estimated that around 10 million Americans have osteoporosis, and about 34 million are at risk of getting this disease. Osteoporosis caused 2 million fractures costing over $19 billion in 2005, and this is expected to rise to 3 million fractures by 2025, costing over $25 billion per year [1]. For load-bearing implants, over 200,000 hip replacements are performed each year in the USA, and this number is increasing steadily due to increased life expectancy [2]. More and more younger patients are in need of total hip replacement (THR) due to increased daily life activities or a more active lifestyle. Thus, the American Academy of Orthopedic Surgeons (AAOS) has categorized musculoskeletal conditions as the number one reason why patients visit a doctor [3]. Considering the tremendous impact of musculoskeletal conditions on our population and economy, the years 2000–10 had been proclaimed as the Bone and Joint

*Corresponding author. Tel.: +1 509 335 7461; fax: +1 509 335 4662. sbose@wsu.edu (S. Bose).

Decade globally; and the years 2002–11 have been marked as Bone and Joint Decade in the USA [4]. The purpose of Bone and Joint Decade is to increase the awareness and advance the understanding of musculoskeletal disorders through prevention, education and research to improve the quality of life for people with musculoskeletal disorders.

A sharp rise in musculoskeletal diseases and disorders often demands a drug treatment at the specific surgery/injury/defect site. In bone tissue engineering, the term “drug” is not limited to only therapeutic agents such as antibiotic, anticancer, anti-inflammatory. The scope of the term “drug” has grown over the last few decades to include growth factors, bioactive proteins, enzymes, and non-viral genes (DNAs, RNAs). Different growth factors, bioactive biomolecules, and drugs are used in bone tissue engineering to induce osteoinductivity in the implanted biomaterials to accelerate the healing process to address various musculoskeletal disorders. Thus, the application of drugs in bone tissue engineering is very wide and a rapidly growing research field of interest.

To be used as a drug carrier, the potential substance must have the ability to incorporate a drug either physically or chemically, retain the drug until it reaches the specific target site, be gradually degraded, and deliver the drug in a controlled manner over time [5]. All these criteria are well met by calcium phosphates (CaPs), and as a result, these materials are promising candidates for drug delivery applications. CaPs are widely used in bone tissue engineering for hard tissues such as teeth or bone replacement, augmentation, and/or regeneration due to their excellent bioactivity and compositional similarities to bone mineral [6–10]. Table 1 [11] shows the typical composition of the inorganic phase of adult human calcified tissues. Dynamic and highly vascularized bone tissue can be viewed as a composite made from biopolymer (mainly collagen) and bioceramic (CaP). CaP, in the form of carbonated apatite, is the principal mineral content (~69%) of natural bone. The organic matrix (~22%) consisted of proteins, type I collagen (90% of the organic matrix) with some non-collagenous proteins (e.g., proteoglycans), lipids and osteogenic factors (i.e., growth factors, such as bone morphogenetic proteins (BMPs) and vascular endothelial growth factors (VEGFs)) [7,12,13]. The remaining 9% is represented by water. Table 2 [14] shows the organic components of bone and their functions in bone mineralization. Osteoinductivity, a very important property of bone, allows bone to repair and regenerate itself. Though osteoconductive, CaP biomaterials are not osteoinductive [15]. However, it has been shown that osteoinductivity to CaP biomaterials can be introduced by combining these materials with growth factors, bioactive proteins, or osteogenic drugs [16–21].

Versatility, excellent bioactivity, compositional similarities to bone mineral, and tailorable biodegradability of CaPs over other ceramics are some of the reasons that CaP systems are increasingly being explored as drug delivery systems (DDSs) for numerous applications in nanomedicine, orthopedics and dentistry. Drug delivery approaches from CaP systems in the form of nanoparticles, coatings, cements and scaffolds have been discussed in this review. In dimensional perspectives, we can consider CaP coating as a two-dimensional construct, whereas calcium phosphate cement (CPC) and CaP scaffolds can be considered as three-dimensional (3-D) constructs. Fig. 1 shows the approaches for CaPs in drug delivery applications, and some common terms and their meanings are presented in Table 3 [10,14,22,23].

2. Categories of calcium phosphates (CaPs)

Depending on temperature, impurities, and the presence of water, CaPs can exist in different phases [1,24]. Exciting features of CaPs are their excellent bioactivity and biodegradability. All CaPs do not have similar bioactivity, and also do not degrade at the same rate. Bioactivity and degradation behavior generally depend on the Ca/P ratio, crystallinity and

phase purity. Regardless of Ca/P ratio, phase and crystallinity, CaPs are relatively insoluble at physiological pH 7.4; however, they have increasingly high solubility in acidic environments, i.e., below pH 6.5 [25–27]. Among all CaPs, the most acidic and soluble CaP is monocalcium phosphate monohydrate (MCPM). Monocalcium phosphate (MCP) is the anhydrous form of MCPM, and is obtained by heating MCPM above 100 °C. Both MCPM and MCP are not biocompatible due to their highly acidic nature and high solubility. Bioactive calcium-deficient hydroxyapatite (CDHA), sometimes called precipitated hydroxyapatite (PHA), has a very complex chemical structure. The Ca/P ratio in CDHA is generally between 1.50 and 1.67, but a Ca/P ratio outside this ratio is also possible. Bone apatite is similar to CDHA except for the presence of carbonate (CO_3^{2-}) and trace elements, for instance, Na^+, K^+, Mg^{2+}, Sr^{2+}, Zn^{2+} [7,9]. Amorphous calcium phosphate (ACP) is similar to CDHA, while octacalcium phosphate (OCP) and tetracalcium phosphate (TTCP) can be synthesized at a higher temperature than other CaPs. Among various CaPs, HA and β-TCP are the most commonly used phases because of their osteogenic property and the ability to form strong bonds with host bone tissues. Solubility of β-TCP is muchhigher than HA, and thus β-TCP is termed a bioresorbable ceramic [28,29]. Development of biphasic calcium phosphate (BCP)-based biomaterials consisting of HA and β-TCP [30–32] are also of interest to control the degradation properties. Table 4 [10,11,24,33,34] presents a list of different CaPs and their properties.

Apart from different phases, sizes, fabrication and formulation techniques, from an application point of view, CaPs can be categorized as nanoparticles (NPs), coatings, scaffolds and cements. Drug loading and release processes can vary depending on whether it is a NP, coating, scaffold or cement. In this paper, we have reviewed drug delivery approaches from CaP nanoparticles, coatings, scaffolds and cements along with the associated concerns.

3. Calcium phosphate nanoparticles (CaP NPs) in drug delivery

Nanoparticle-based drug delivery systems are a rapidly growing field of interest for effective targeted drug delivery application. Inorganic nanoparticles, such as magnetic iron oxides [35–37], silica [38–40], gold [41–44], and CaPs [26,45–49], have gained attention from the researchers due to their ease of handling, biocompatibility and suitable surface chemistry. However, associated toxicity resulting from different nanoparticulate materials is a serious concern [50–52]. Among many inorganic DDSs, special emphasis is given to CaP NPs because of their superior biocompatibility and biodegradability compared to others. A great advantage of using CaP NP is that it is found throughout the body, as it is the major constituent of bone and tooth enamel. Synthesis of CaP NPs is an intimate part of drug loading or incorporation processes. Synthesis of CaP NPs can be done by various methods such as wet precipitation [53–56], solid state reaction, sol–gel [57–60], flame spray pyrolysis [61], hydrothermal [62], spray-drying [63], micelle mediated [64], reverse micelle mediated [65–67], and double emulsion mediated synthesis [68].

For many drug carriers, biodegradation of the carrier prior to delivery of the drug at the target site can also pose a threat to the patient. Major concerns associated with biodegradable polymeric nanoparticles are the acidic or degradation by-products that can alter the drug activity, and even can adversely interact with the drug or tissue as they come in contact during circulation. Degradation products of CaPs are Ca^{2+} and PO_4^{3-}, which are already inherent to the body, and both Ca^{2+} and PO_4^{3-} ions are also found in relatively high concentrations (1–5 mM) in the bloodstream [69]. This natural occurrence of CaP is one of the primary advantages over other synthetic drug delivery systems, which might trigger an immunogenic response. The success of a DDS depends on its effective delivery of drug/

therapeutic agent at the targeted site. Regardless of the Ca/P ratio, phase and crystallinity, CaPs are relatively insoluble at physiological pH 7.4; however, they have increasing solubility in acidic environment, e.g. below pH 6.5 [25–27] such as in endocytic vesicles [70], lysosomes [71] or around solid tumors [72]. Moreover, CaPs are not prone to enzymatic degradation in the physiological environment, unlike organic or polymeric DDSs [73,74]. Thus, non-immunogenic response, non-toxic degradation products, and pH-dependent solubility make CaPs also suitable for intracellular imaging and drug delivery applications [75,76] in the form of NPs in addition to being a bone substituent. Fig. 2 shows a schematic of CaP NPs for drug delivery applications.

Rapid clearance from the body and extracellular enzymatic degradation by plasma nucleases are the major reasons that make direct gene delivery an inefficient process [77,78]. Naked DNA and siRNA are negatively charged, and the electrostatic repulsion with the anionic cell membrane further reduces their transfection efficiency [79]. Therefore, a suitable delivery vehicle is necessary for effective transfection. Though viral gene delivery is very widely used, non-viral gene delivery is getting significant attention due to safety concerns associated with viral gene delivery, such as immunotoxicity, intercellular trafficking, and possibility of mutation [80]. CaP NPs have proven to be effective for non-viral intracellular gene delivery or transfection [27,81,82], and gene silencing through small interfering RNAs (siRNAs). DNA or RNA binding to CaP NPs occurs through electrostatic interaction between Ca^{2+} in CaP carrier and phosphate groups in DNA or RNA structure [83]. Fig. 3 shows the schematic of the interaction of a nucleic acid on the CaP NP surface [84]. In intracellular gene delivery method, the genes are delivered to tumor/cancer-specific cells. These genes can then kill the cells by replacing the existing genes, or may promote certain enzyme activity that is capable of inducing cytotoxicity to the cells. Zhang et al. [85] studied *in vitro* and *in vivo* therapeutic effect of a CaP NP mediated carcinoembryonic antigen-cytosine deaminase (CEA-CD) delivery, where an enhanced CEA promoter was fused to a suicide gene, cytosine deaminase (*CD*), to treat colon cancer. 5-fluorouracil (5-FU) is a prodrug that converts into a cytotoxic drug, 5-fluorocytosine (5-FC), when deaminated by CD. CEA is a tumor tissue specific promoter, and is overexpressed in most colon cancer. CEA was used by Zhang et al. to reduce the side-effects. CaP NPs were used because of their lack of toxicity and high transfection efficiency. CEA-CD was efficiently delivered by CaP NP both *in vitro* and *in vivo*. CPNP/CEA-CD/5-FC efficiently induced cytotoxicity in CEA-positive cells and triggered cancer cell death. Fig. 4 shows a schematic representation of gene delivery into cell nucleus through a double-shell CaP NP. Cellular uptake of CaP NPs loaded with DNAs/RNAs is caused by endocytosis through lipid bilayer cellular membrane. DNAs or RNAs escape from the endosome following the dissolution of CaPs in the acidic environment of the endocytic vesicle. Degradation of DNAs/RNAs by lysosomal nucleases could limit the transfection efficiency if endosomal escape of DNAs/RNAs could not occur before the fusion of endosome with lysosome. Production of certain enzymatic activity, or a stop in synthesizing certain genes, are triggered once the delivered DNAs/RNAs are transported into the cell nucleus through the nuclear membrane. CaP chemistry, surface area, surface charge, and crystallinity also play a great role in gene loading efficiency. Hanifi et al. [58] showed that Mg^{2+} doping into HA increases the surface positive charge of the CaP NPs and hence increased its DNA loading capacity. They also showed that the presence of β-TCP phase into HA increased gene delivery properties by increasing its solubility inside endosome.

Tissue/cell imaging is also possible by CaP NPs doped with lanthanum [86–89] or surface functionalized by organic dye molecules [75,76,90–92]. Lanthanum doping or surface functionalized dyes can act as fluorescing probes. Indocyanine green (ICG) is a FDA (US Food and Drug Administration) approved near infrared (NIR) organic dye that can be used in deep tissue imaging. Its application is limited by low quantum yield, photoleaching effect,

and nonspecific quenching. Low retention capability, and minimum protection against ICG dimerization, were observed with polymer-based careers. To address these limitations of ICG with other careers, Altinoglu et al. [93] embedded ICG into CaP NPs (16 nm average diameter) for sensitive deep-tissue NIR imaging. As-synthesized ICG doped CaP NPs contained surface functionalized carboxylate or polyethylene glycol groups. No adverse effects were observed on the optical properties (absorption and emission) of the ICG doped colloidally stable CaP NPs. 200% greater quantumefficiency, 500% longer photostability relative to free dye were observed from these ICG doped CaP NPs. A prolonged (up to 4 days) fluorescence signaling was observed from ICG doped CaP NPs compared to free ICG (<24 h) in an *in vivo* nude mice model. A short fluorescence was attributed to rapid aggregation of free dye molecules in physiological condition, and rapid clearance from the body.

Simultaneous drug delivery and bio-imaging by a fluorescing probe was studied by Kester et al. [75] and Banerjee et al. [92]. Kester et al. [75] encapsulated water-insoluble hydrophobic decanoyl ceramide (Cer_{10}), an anticancer drug, and rhodamine-WT (Rh-WT) dye into hydrophilic CaP NPs through double reverse-micelle approach. Rhodamine-WT (Rh-WT) dye embedded within the resulted 20 to 30 nm diameter CaP NPs was used as a fluoroprobe for bioimaging. Successful delivery of hydrophobic Cer_{10} was shown by the reduced survival of melanoma and breast cancer cells as compared to CaP NPs containing fluorophore without Cer_{10} as control. Thus, CaP NPs could be very promising for targeted delivery of hydrophobic drugs like ceramide, which is not possible to administer through aqueous formulation [75]. In another study, a pH-sensitive release of Alendronate (AD) from CaP NPs is reported by Banerjee et al. by synthesizing CaP-AD nanoconjugate [92]. AD is a bisphosphonate (BP) drug, which is used for bone diseases like osteoporosis. Bisphosphonates (BPs) are a group of synthetic drugs with a structural backbone similar to inorganic pyrophosphate. The synthesized CaP-AD nanoconjugate surface was further modified by rhodamine-B (RDB) dye. An average dimension of 20 nm × 44 nm and 21 nm × 44 nm of CaP-AD and CaP-AD-RDB nanocomposites, respectively, were reported. A significant controlled alendronate release was observed at pH 5, which is the pH around solid tumors or in endolysosomes, as compared to pH 7.4, which is the physiological pH. High AD release at pH 5 was correlated with the high dissolution of CaP at this pH shown by Ca^{2+} ion measurement as shown in Fig. 5. CaP-AD nanocomposites were also effective in decreasing osteoclast cells activity compared to bare CaP nanoparticles measured by TRAP expression, a marker for osteoclasts phenotype. Osteoclast cells resorb bone mineral during the bone remodeling process. Cheng and Kuhn [46] synthesized CaP NPs (HA) conjugated with *cis*-diamminedichloro- platinum (CDDP, cisplatin), a commonly used chemotherapy drug with high antitumor activity. A sustained release of the drug, 30% of the conjugated drug in 16 days, was observed from CDDP conjugated CaP NPs. Cytotoxicity test in cancer cell showed conjugation of CDDP with CaP NPs, and its subsequent release did not significantly alter drug activity compared to free drug.

The use of CaP particle systems for protein delivery has also been studied using model protein bovine serum albumin (BSA). Dasgupta et al. [67] showed that protein loading and release from CaP NPs depends on the particle size, surface area, and phase composition of CaPs, where CaP NPs were synthesized using a reverse micro-emulsion technique followed by BSA loading. In another study, Dasgupta et al. [94] incorporated BSA into Zn and Mg doped HA NPs synthesized by an in situ precipitation process. Surface charge effect, similar to reported by Hanifi et al. [58], on protein incorporation was observed. Increased BSA loading was due to the c-site lengthening effect by the dopant in the HA crystal lattice; this is shown in Fig. 6a. Addition of dopants increased the protein uptake compared to the undoped HA NPs. Undoped, Zn-, and Mg-doped HA NPs showed BSA uptake of 18 wt.%, 24 wt.%, and 21 wt.%, respectively. A two-stage release characteristic was observed, as

shown in Fig. 6b, where the first step was due to the loosely bound BSA released from the CaP surface, and the second step BSA release was due to dissolution of the CaP NPs into the solution. Thus, the choice of a dopant with high charge density can lead to attaining CaP NPs with high surface charge, which apparently has an immense impact on protein, gene, and/or drug loading on these NPs.

3.1. Challenges with CaP NPs

Though by definition, NPs are considered to be equal to or less than 100 nm, particle size between 10 and 200 nm is suitable for drug delivery applications based on *in vivo* studies [50]. However, beyond a particle size range nanoparticles may show some toxicity *in vivo* through excess delivery of Ca^{2+} ions into cells. Synthesis of CaP NPs and maintaining the size after drug conjugation/incorporation/adsorption is a critical challenge. Storage of CaP NP transfection solution is also a critical challenge because NPs grow bigger with time into microcrystals [95], and transfection efficiency is also dependent on the particle size [26]. Intracellular degradation of the CaP NPs into lysosome before entering the nucleus decreases the transfection efficiency. Development of multi-shell CaP NPs is a potential approach to address this issue. Sokolova et al. [95] coated the core CaP with DNA followed by coating with CaP, and finally a DNA coating. It was shown that a significant increase in transfection efficiency was attained by this type of multi-shell CaP NPs as compared to single layer DNA coating as shown in Fig. 7. Increased transfection efficiency by double-shell and triple-shell DNA-CaP NP conjugate was reported due to the increased protection and stability of DNA-CaP NP conjugate from extra- and intracellular degradation processes. Increased protection and stability of DNA-CaP NP conjugate was more dominant than the charge effect, as shown in Fig. 7 between double-shell and triple-shell DNA-CaP NP conjugates.

4. Drug delivery from CaP coatings

Due to their bioinert nature, metallic implants have poor osteoconductivity. Moreover, fibrous tissue encapsulation around the implant poses a serious threat to the long term activity of the implant. CaP coating onto metallic implant had been introduced to initiate a bioactive fixation after surgery, and to increase the long term activity. Post-surgery periprosthetic infections still remain a threat during setting of total joint arthroplasty, pose a serious threat to the short and long term stability of the implant in orthopedic surgery [96,97], and may also lead to a second surgery [98,99]. This challenge could be addressed by local delivery of antibiotic drug from the coated implant. Local drug delivery at the respective targeted site is also used in the field of medicine other than musculoskeletal disorder treatments, and has been proven very effective against systemic delivery [100,101]. A high dose concentration of the drug is usually required for systemic delivery compared to local delivery, and yet the effective concentration at the target site may not be enough for effective and permanent cure [98]. Local drug delivery ensures delivery of the drug to the surrounding tissue at the target site, which reduces associated toxicity to other non-target sites [100,102,103].

Although orthopedic-related bacterial infections are well treated by various antimicrobial agents, an increasing antibiotic resistance is an alarming concern [104]. Silver can effectively be used as antimicrobial agent against a broad range of Gram-positive and Gram-negative bacteria, and bacterial resistance against silver is also minimal [104,105]. Silver shows its bactericidal effect at a minimum concentration of 35 ppb (parts per billion) without any toxicity to mammalian cells [99]. The efficacy of local delivery of silver ion (Ag^{+}) from CaP coating on titanium has been tested by Roy et al. [106] against *Pseudomonas aeruginosa* and *Pseudomonas aureus*, which are known to cause post-operative infections. Laser engineered net shaping (LENS™) was used to coat TCP onto Ti.

Silver (Ag) was electrodeposited from 0.001 M, 0.1 M, and 0.5 M $AgNO_3$ solutions, respectively, on CaP-coated titanium (Ti) samples. Samples coated from 0.001 M $AgNO_3$ solution were not very effective for the reduction of bacterial colony growth. Although samples coated from 0.1 M and 0.5 M $AgNO_3$ solutions were effective in 99.99% reduction of bacterial colony growth after 24 h, samples coated from 0.5 M $AgNO_3$ solution showed toxicity to osteoblast cell proliferation. Ag concentration 0.1 M for electrode-position was found to be optimum for osteoblast cell proliferation without any cytotoxicity, and there was significant reduction (99.99%) of *Pseudomonas aeruginosa* and *Pseudomonas aureus* bacterial colony growth on the Ag-CaP surface compared to CaP coating without Ag.

Biomimetic coating or mineralization is a technique in which an osteoconductive amorphous calcium phosphate (ACP) layer is introduced on the surface of a substratum immersed in a supersaturated simulated body fluid (SBF) solution. The ion concentrations of SBF solution are similar to human blood plasma, and the ACP that forms in SBF is calcium deficient carbonated hydroxyapatite (CDCHA). Table 5 shows the ion concentration comparison between SBF and blood plasma adapted from Kokubo and Takadama [107]. Instead of simple surface adsorption, co-precipitation of drug or osteogenic growth factor molecules during biomimetic coating is also gaining significant attention from the scientific community [108]. Fig. 8 shows a schematic of biomimetic precipitation and biomimetic co-precipitation. Biomimetic co-precipitation of a series of antibiotics such as cephalothin, carbenicillin, amoxicillin, cefamandol, tobramycin, gentamicin and vancomycin, on titanium alloy (Ti6Al4V) was done by Stigter et al. [109]. They examined release kinetics in PBS of 7.4 pH at 37 °C, and the efficacy against *Staphylococcus aureus* of these antibiotics. A thin ACP layer was precipitated from a five times concentrated SBF solution [110] for 24 h, followed by biomimetic coprecipitation of antibiotics from a supersaturated SBF solution [111] for 48 h at 37 °C. Fig. 9a [109] shows the antibiotic concentration in the coating with the variation of concentration in coating solution. Antibiotic incorporation efficiency into coating was anticipated to have a relation with the presence or absence of carboxylic (COO^-) group, and their interaction with calcium ion (Ca^{2+}) present in the coating solution. The chemical nature and concentration of these antibiotics had a significant influence on the carbonated hydroxyapatite (CHA) coating thickness formed by the biomimetic technique. Release behavior is shown in Fig. 9b [109]. The release of antibiotics was controlled by their chemical nature, i.e., acidic or basic, molecular size, and the diffusion rate into release medium.

Complications such as delayed healing or non-unions of bone fractures in orthopedic and trauma surgery can be addressed by the exogenous application of growth factors to stimulate bone healing. Thus, growth factors have also been applied on CaP-coated orthopedic and dental implants to induce osseointegration, and accelerate the reestablishment of full functionality. Liu et al. [16] studied the effect of biomimetically coprecipitated bone morphogenic protein (BMP-2), an osteogenic growth factor, on bone formation at an ectopic site in rat model up to 5 weeks. An ACP layer was created on Ti alloy (Ti6Al4V) disks (1 cm in diameter) from a five times concentrated SBF solution at 37 °C for 24 h followed by biomimetic coprecipitation of BMP-2 from a supersaturated CaP solution of pH 7.4 at 37 °C for 48 h. Naked Ti alloy disk, and Ti alloy disk with CaP coating (no BMP-2) as negative controls; and Ti alloy disk with CaP coating and superficially adsorbed BMP-2 as positive control, were used. Biomimetically coated samples had 1.7 ± 0.079 μg BMP-2/sample, where superficially adsorbed BMP-2 group samples had 0.98 ± 0.045 μg BMP-2/sample. Ti alloy samples with biomimetically coated BMP-2 showed a sustained and increased ossification over the 5-week time period compared to superficially adsorbed BMP-2 samples, which showed only a transient (1 week) osteogenic response. The sustained osteogenic activity from the biomimetically coated BMP-2 was hypothesized due to the

gradual release as opposed to the short burst release from the surface adsorbed BMP-2 groups.

Bisphosphonates (BPs) are a group of synthetic drugs with a structural backbone similar to inorganic pyrophosphate as shown in Fig. 10. BPs are widely used in skeletal disorders, including osteoporosis, Paget's disease, and tumor-associated osteolysis and hypercalcemia [112–114]. BPs inhibit osteoclast (bone resorbing cells) activity, and that's why BPs are also known as antiresorptive agents. Systemic delivery of BPs by oral administration or intravenous injection often causes side-effects like fever and/or throat or stomach ulcers. Moreover, bioavailability of BPs is also very low [115]. Local BP delivery can also induce early stage osteogenesis, in addition to reducing the risk of bone fracture from osteoporosis, by inhibiting osteoclast activity. This causes improved mechanical interlocking of the implant with the surrounding host bone tissue, and faster recovery from surgery. Peter et al. [116] introduced zoledronate, a member of the BP family, on the HA-coated titanium implant (3 mm (h) × 5 mm (Ø)) to study the effect of local zoledronate delivery on mechanical fixation of the implant and host bone, which increased bone formation. A 20 μm thick fairly crystalline (62%) HA coating was prepared by a plasma spray technique. HA-coated Ti implants were inserted in rat condyles with various zoledronate concentrations, 0.0 μg (control), 0.2 μg, 2.1 μg, 8.5 μg, and 16 μg, respectively, per implant. A zoledronate concentration dependant increased mechanical fixation, and increased peri-implant bone density was also observed. Zoledronate concentration 2.1 μg/implant produced the highest peri-implant bone density, and mechanical fixation compared to other concentration and control (without zoledronate). Garbuz et al. [117] studied the effect of porous tantalum coated with microporous CaP with alendronate on new bone formation in the gap between implant and host bone; and compared with uncoated porous tantalum implant, and CaP-coated porous tantalum implant without any alendronate. Microporous (200–300 nm pore size) CaP coating on porous tantalum (400–500 μm pore size) was performed by electrolytic deposition technique and alendronate immobilization was carried out by soaking the coated implant in phosphate buffer solution (PBS) containing alendronate. Alendronate concentration of 1.37 μg per tantalum implant (8 mm (h) × 3.18 mm (Ø)) was used. A significant bone ingrowth was observed on alendronate - CaP-coated microporous tantalum implant using rabbit femur model. The presence of alendronate disrupted osteoclast activity and enhanced osteoblast activity. Porous tantalum implants coated with CaP and alendronate (Ta-CaP-ALN) showed significantly more gap filling, bone ingrowth, and total bone formation than the group treated with the uncoated porous tantalum implants (Ta), and the group treated with the CaP-coated implants (Ta-CaP).

4.1. CaP coatings: challenges

The success of a coated implant depends on the stability of the coating. Stability of the coating is controlled by its physical and mechanical properties such as crystallinity, phase composition, dissolution characteristics, coating thickness and coating strength. Coating techniques such as dip coating [118], sol–gel [119,120], electrophoretic deposition [121,122], biomimetic coating [16,108, 123], simultaneous vapor deposition [124], pulsed laser deposition [125], laser processing [126,127] and plasma spraying [128,106] have been used for ceramic coating on metals. Although dip coating, sol–gel, electrophoretic deposition and biomimetic coatings are suitable for coating a complex shape, all these techniques suffer from weak coating strength. In spite of being a line-of-sight technique, simultaneous vapor deposition, laser processing, pulsed laser deposition and plasma spraying offer some advantage on interfacial strength and crystallinity over other techniques. Although CaP coating makes a metallic implant bioactive by inducing osteoconductivity, osteoinductivity can only be induced by osteogenic drug or growth factors. Since almost all coating techniques involve high temperature in-processing or post-processing, any kind of

drug or growth factors are only introduced after the coating process is done and mostly by adsorption [102,116,129]. This leads to a potential burst release effect of the loosely bonded drugs or growth factors. Radin et al. [102] loaded vancomycin on a CaP-coated titanium alloy substrate by only vancomycin adsorption (i), and vancomycin adsorption followed by lipid coating onto it (ii). A prolonged release of the drug, resulting up to 72 h bacterial inhibition, was reported from lipid-coated samples as compared to 24 h bacterial inhibition from non-lipid-coated samples. Thus, a thin biodegradable polymer coating after drug adsorption could be a potential solution to address the initial burst release, provided that this polymeric coating does not adversely affect or reduce the bioactivity of the coating.

5. CaP scaffolds in growth factor delivery

A scaffold is defined as a structure that allows cells and extracellular matrices to interact, and provides the mechanical support for growing cells and tissues. In an ideal case, a CaP scaffold would eventually degrade while the newly formed tissue takes over the space. The degradation rate of these CaP scaffolds depends on the solubility of the type of CaP. A scaffold can have two types of porosity: macroporosity (pore size > 50 μm) and microporosity (pore size < 10 μm) [130]. The presence of porosity, particularly interconnected porosity, provides higher surface area for improved mechanical interlocking between the scaffold and surrounding host tissue [131,132]. Interconnected porosity also provides pathways for micronutrients [133]. Growth hormones (GHs), growth factors (GFs), bone morphogenetic proteins (BMPs), and/or mesenchymal stem cells (MSCs) can improve the biological properties of porous scaffolds further, either by inducing osteogenesis or angiogenesis through osteoinduction or vascularization, respectively. Table 6 [134–136] presents some commonly used growth factors in tissue engineering for drug delivery applications.

GHs have a stimulatory effect on osteoblast proliferation and differentiation [137], and thus play a vital role in bone formation and remodeling [137,138]. Effect of human growth hormone (hGH) on *in vivo* bone growth and CaP resorption by localized delivery from a macroporous biphasic calcium phosphate (MBCP: with a 60/40 weight ratio of HA/β-TCP) in rabbit model was studied by Guicheux et al. [139]. Mean macropore diameter and macroporosity of these scaffolds were 565 ± 33 μm, and 50%, respectively. A 50 μl solution containing 0.1 μg, 1 μg, and 10 μg of hGH, respectively, was loaded on the cylindrical MBCP samples with 6 mm(h) × 6 mm(Ø) dimension. Significant increase in bone growth (65%) and CaP resorption (140%) is reported due to hGF as compared to control (with no hGH). A 36%, 65%, and 35% bone ingrowth was observed for 0.1 μg, 1 μg, and 10 μg of hGH, respectively. Scaffolds loaded with 1 μg hGH stimulated significant bone ingrowth and ceramic resorption compared to scaffolds with 0.1 μg and 10 μg of hGH. Thus there is an optimum in terms of hGF amount to achieve significant bone growth within the scaffold which is also controlled by CaP resorption.

Hepatocyte growth factor (HGF) induces angiogenesis by promoting VEGF expression [140]. It has been shown that HGF induces osteoblast proliferation and further increases the bioactivity of CaPs [141]. Hossain et al. showed an enhancement of osteoblast differentiation when cultured on HGF adsorbed HA-based CaP compared to CaP without any HGF [142]. They have also tested the attachment efficiency of HGF on dense HA scaffolds by two different procedures. All samples were incubated at 4 °C for 24 h after placing 100 μl HGF solutions in PBS containing 200 ng HGF. After 24 h, one set of samples were kept at room temperature and allowed to dry over 6 h, and another set were kept at 4 °C for another 24 h by adding PBS. Approximately 30% of the total HGF placed on the HA surface was adsorbed, when the solution was allowed to dry; almost 50% was adsorbed after 48 h incubation.

Takahashi et al. [20] showed that the addition of rhBMP-2 to porous HA grafts (40% porosity with pore size ranging from 100 to 500 μm) enhances the rate of anterior cervical fusion through osteogenesis using goat anterior cervical fusion model. Two different rhBMP-2 dosage, 5 μg and 50 μg per implant, were tested. Although 5 μg rhBMP-2 group induced a significant osteogenesis compared to the control group without any rhBMP-2, application of an adequate amount rhBMP-2 rather than a low dose was suggested. Koempel et al. [143] showed that human recombinant bone morphogenetic protein-2 (rhBMP-2) can promote the implant– host tissue integration by adsorbing rhBMP-2 on macroporous HA, and implanted in the subperiosteal pockets created on rabbit skull. Commercially available HA scaffolds with 40% porosity and 100–300 μm non-interconnected macropores were used. Many studies showed that the presence of macropores in CaP scaffolds loaded with BMP had a significant effect on new bone formation [139,143,144]. An insignificant effect of macropores loaded with BMP is also reported by Levengood et al. [145]. The presence of microporosity in a scaffold is undoubtedly beneficial for new bone formation. Woodard et al. [146] showed that the presence of microporosity (2–8 μm) in HA scaffold improved osteoconductivity as compared to scaffolds without any microporosity. Increased growth factor retention by rhBMP-2 due to the presence of microporosity was observed in scaffolds. Polak et al. [147] showed that the presence of microporosity accelerated the healing process twice as fast as compared to scaffolds without any microporosity. They also showed that the addition of BMP-2 in microporous CaP samples accelerated the healing process four times as fast as compared to scaffolds without any BMP-2.

Bone marrow stromal cells (BMSCs) are capable of self-renewal and differentiation into various osteogenic lineage cells, including chondroblasts and osteoblasts, and are considered as progenitors of skeletal tissue system [148,149]. Martin et al. [150] investigated the influence of a series of growth factors on the growth and bone formation capability from BMSCs. In *in vitro* conditions, they showed that endothelial growth factor (EGF) and fibroblast growth factor (FGF-2) influenced BMSC growth significantly, while dexamethasone (DEX) and FGF-2 promoted significant bone formation from BMSC. In an *in vivo* mice model, they also showed that BMSC seeded on CaP induced bone formation compared to control collagen sponge seeded with BMSC, where no bone formation was observed. HA scaffolds with 70–80% porosity were used with a pore distribution:<10 μm, ~3% vol; 10–150 μm, ~11% vol; >150 μm, ~86% vol. The effect of BMP-7 combined with VEGF and MSCs on osteoinduction in a porous BCP scaffold was investigated by Roldan et al. [151]. The weight ratio of HA/TCP in the BCP scaffolds was 60/40 with 92–94% volume fraction porosity, and interconnected macropore size 360–440 μm and 900–1100 μm, and 0.4–4 μm micropore size. Fig. 11i shows the images of this BCP scaffold and its strut. Though only the BMP-7 group showed the highest new bone formation, no statistically significant differences were observed in new bone formation in the presence of BMP-7/VEGF, BMP-7/MSCs compared to BMP-7 alone in these scaffolds. The control ceramic (with no BMP-7) scaffold also showed considerable new bone formation. The osteoinduction in the control ceramic was induced by the presence of micro- and macropores. Fig. 11ii shows the difference in new bone formation due to the presence and absence of BMP-7 in the BCP scaffolds.

Kundu et al. [152] reported the superiority of HA with lower pore percentage with a distribution of mainly micro-pores over the higher pore percentage both *in vitro* and *in vivo.* They treated chronic osteomyelitis caused by β-lactamase-producing strains using a combination of sulbactam sodium (SUL, a β lactamase inhibitor) and ceftriaxone sodium (CFT, a β-lactam antibiotic) in osteomyelitis induced rabbit model. HA scaffolds with lower and higher pore percentage were characterized with 50–55% porosity with ~110 μm average pore size and higher interconnectivity (10–100 μm); and 60–65% porosity with ~140 μm average pore size and lower interconnectivity (30–120 μm), respectively. Drug adsorption

was carried out by soaking the scaffolds in a drug solution of 500 mg ml^{-1} with a 2:1 ratio of CFT and SUL.

5.1. CaP and polymer composite scaffolds

Biodegradable polymers are very frequently used with CaP polymers to make ceramic–polymer composite scaffolds to improve mechanical properties. Polymer coatings on CaP ceramic scaffolds are often applied to improve brittleness and weak strength. In drug delivery applications, polymer coating is also applied to the drug-adsorbed surface of the ceramic scaffold to control the drug release behavior. Sometimes, drugs are also impregnated into the polymer coating [153,154], and recently an increasing interest has been paid to functionalization of polymeric coatings [155,156] to induce hydrophilicity, for better drug interaction, or to make covalent bonding with the drug.

Kim et al. [157] coated HA scaffolds having ~87% porosity and 150–200 μm pore size, made by polyurethane foam reticulate method, with a mixture of HA powder and polycaprolactone (PCL) polymer. Coating was done by the dipping-drying process with varying concentration and HA/PCL ratio. The antibiotic drug tetracycline hydrochloride (TCH) was mixed with the HA/PCL coating mixture in dichloromethane. An increase in compressive strength and elastic modulus was achieved by this coating, where an increase in compressive strength from 0.16 ± 0.04 MPa to 0.45 ± 0.04 MPa, and elastic modulus from 0.79 ± 0.04 MPa to 1.43 ± 0.2 MPa, respectively, were observed for 3.75% PCL (w/v) concentration in coating solution. A constant drug-to-matrix ratio (TCH/HA + PCL = 0.1) was maintained in all coating solutions. Drug release was dependent on the coating dissolution from the scaffold, where the dissolution rate was highly dependent on the HA/PCL ratio. A decreasing trend in the percentage drug release was observed with increasing PCL concentration in the coating solution. Approximately 20–30% of the loaded drug was released during initial 2 h in PBS, while 40–60% of the loaded drug was released in 7 days depending on the coating composition. Xue et al. [153] demonstrated a sustained and controlled protein delivery from β-TCP scaffolds with PCL coating, where strength was improved due to PCL coating and model protein bovine serum albumin (BSA) release kinetics was studied. Fig. 12 shows morphologies and release profiles of the uncoated and PCL-coated β-TCP scaffolds. Polyurethane foam reticulate method was used to fabricate TCP scaffolds with 70–90% porosity and 300–800 μm interconnected macropore size. An increase in compressive strength was observed with increasing PCL concentration. Compressive strength was decreased with increased percentage porosity. BSA was encapsulated efficiently within the PCL coating without significant denaturation. BSA encapsulation can be controlled by varying protein composition in PCL coatings. Rai et al. [154] studied drug loading and release behavior of PCL-TCP biodegradable composite scaffold fabricated by fused deposition modeling for bone regeneration. Fibrin sealant was used to promote the loading efficiency of rhBMP-2 onto the PCL and PCL-TCP composites. It was reported that PCL-TCP- fibrin retained rhBMP-2 longer than PCL-fibrin composites, and interpreted that this was likely due to the formation of intermolecular linkages between rhBMP-2 and TCP. Yoshida et al. [21] studied the effect of rhBMP-2 on new bone formation in surgically created defects in rabbit mandibles. Porous HA scaffolds were coated with rhBMP-2 and atelopeptide type I collagen. A significant early stage new bone formation, due to osteoinduction from rhBMP-2, was observed compared to the control group (HA coated with only atelopeptide type I collagen).

5.2. CaP scaffolds: fabrication, drug loading and critical issues

Along with biological and mechanical properties, architectural features are also important for scaffolds used in tissue engineering application. 3-D interconnected pores are essential for scaffolds for better cell adhesion, mechanical interlocking between host tissue and

scaffold, and flow transport of nutrients and metabolic waste [132,158–161]. The scaffold should also have enough temporary strength to withstand *in vivo* stresses and loading at the site of application until newly formed bone replaces the biodegradable scaffold matrix [162]. Many conventional techniques such as impregnation and sintering, fiber bonding, solvent casting and particulate leaching, gas foaming, thermally induced phase separation are available for scaffold fabrication [163,164]. The fabrication of CaP-based scaffolds with complex architectural features is difficult by conventional techniques as precise controlling of pore size, pore distribution, pore interconnectivity and percentage porosity cannot be maintained by conventional techniques [165,166]. Unlike conventional techniques, the solid freeform fabrication (SFF) technique allows flexibility in designing and manufacturing scaffolds with complex geometry [165,167–172]. SFF is a layer-by-layer manufacturing technique. This technique directly uses computer aided design (CAD) data file to fabricate the scaffold. Among many existing SFF methods, selective laser sintering (SLS), stereolithography (SLA), fused deposition modeling (FDM) and three-dimensional printing (3DP) are the most widely used [132,164,168]. Fig. 12(c) shows a schematic of 3D printing along with 3D printed interconnected macro porous scaffolds with different pore sizes, and some other 3D printed parts fabricated at Washington State University using a 3D printer (ProMetal®, ExOne LLC, Irwin, PA, USA). In most cases, CaP scaffolds are subjected to post-processing high temperature sintering to achieve high density and sufficient mechanical strength. That is why any drug/biomolecules cannot be incorporated into CaP scaffolds before high temperature densification – unlike CPCs, where post-processing sintering is not required and setting takes place at the physiological temperature. Thus, drugs/biomolecules are applied by adsorption, entrapped into or immobilized on the polymeric coating on the sintered ceramic scaffold. Hence, polymeric degradation by-products and their interaction with the physiological system also need to be considered before applying any polymeric coating. Fig. 13 shows a schematic representation of drug loading approaches on CaP scaffolds or coatings. Treatment approaches designing depends on the requirements, type of drugs/biomolecules under consideration and their interactions with CaPs.

5.3. Release behavior from CaP scaffolds

Fig. 14a and b illustrates the schematic of drug release from CaP scaffolds, where drugs are adsorbed on the CaP scaffolds. Scaffolds can have micropores or macropores or both. Drug release depends primarily on chemical and electrostatic interaction between CaPs and drug molecules as well as the environment. Fig. 15 shows a schematic of a chemical interaction between a BP drug molecule and calcium deficient apatite (CDA), a CaP [173]. An initial burst release can occur when the drug is adsorbed only by electrostatic interactions. Drug release can also be dependent on the dissolution/degradation rate of CaP, when there are chemical interactions between drug molecules and CaPs. Sometimes polymer coating is done to attain a sustained release and prevent any burst release. Drug or protein molecules can also be impregnated into polymer coatings. Drug release from polymer-coated CaP scaffold is dependent on the diffusion of drug molecules through polymer coating, and degradation of coating. Percentage porosity, pore size, presence of intrinsic micropores, and pore interconnectivity – all these factors can have a vital impact on drug adsorption efficiency and release behavior. An increase in drug adsorption efficiency (~48% adsorption for 50% porosity and ~82% for 60% porosity) was observed with an increase in percentage porosity due to the increased surface area by Kundu et al. [152]. An initial burst release was observed in all cases. A faster elution rate was observed from a high percentage porosity sample. The presence of high volume fraction porosity and a bigger size of macropores facilitated the diffusion of drugs at a faster rate than the samples with lower volume fraction porosity and smaller macropore size. Fig. 16 presents the release profile of 1 μg hGH loaded on MBCP scaffolds for up to 9 days from the study done by Guicheux et al. [139]. A first order diffusion controlled initial release was predicted from the linear pattern of cumulative

release vs. square root of time curve. Ceramic resorption mediated release was also predicted in addition to diffusion.

6. Calcium phosphate cement (CPC)

In the 1980s, LeGeros [174] and Brown and Chow [175] introduced the CPC formulation. CPC refers to the solid CaP formed from semi-solid or paste form. The semi-solid or paste is obtained by mixing CPC powder and a liquid called cement solution. The CPC powder is usually a mixture of two or more than two different CaPs, while the liquid can be only water or an aqueous solution. The hydrolysis reaction, upon mixing of CPC powder and liquid, leads to set and harden the cement by a combination of dissolution and precipitation process [176]. The possible reaction products of CPCs are brushite (DCPD), hydroxyapatite (HA) or calcium deficient hydroxyapatite (CDHA) [177]. The injectibility of CPC paste allows it to fit the bone defect or bone cavity perfectly. Another great advantage of CPCs their is low temperature *in vivo* self-setting capability without causing any harm to the surrounding tissue. Properties of CPCs such as mechanical strength, setting time, porosity, and swelling can be controlled by liquid-to-powder ratio, pH of the liquid phase, chemistry, crystallinity, particle size, and the presence of nucleating agents in the reaction system [178– 182].

In addition to acting as bone substitute, CPCs can also be used for local drug delivery for the treatment of different skeletal diseases such as bone tumors, osteoporosis or osteomyelitis. The highly microporous structure of CPC, after setting, allows it to incorporate drugs into its structure. Fig. 17 shows the presence of two different types of porosities, resulting from the distance between crystallites and aggregates [183]. The drug can be introduced either in the liquid or the solid phase of the CPC, but care must be taken that the physicochemical properties of the drug or protein do not change during the chemical reaction and setting of CPC. Different kinds of drugs, including antibiotics [184–186], anticancer agents [103], growth factors [17], proteins/amino acids [18,19], and antimicrobial peptides (AMPs) [187,188], have been incorporated into CPCs for various applications.

The influence of alendronate (AD) into the CPC matrix on cement setting time, compressive strength, drug release kinetics, and bioactivity was investigated by Jindong et al. [189]. Three different AD concentrations, 2, 5 and 10 wt.% into CPC matrix, and a control (CPC with no AD), were used. Both the initial (setting time for control: 10.1 ± 0.74 min; CPC with 10 wt.% AD: 29.8 ± 1.92 min) and final (setting time for control: 23.7 ± 1.20 min; CPC with 10 wt.% AD: 47.8 ± 2.39 min) setting time was increased with increasing AD concentration. A significant reduction in compressive strength was also observed with AD incorporation into CPC matrix (CPC control: 13 ± 0.595 MPa, 2% AD: 5.16 ± 0.268 MPa, 5% AD: 5.54 ± 0.233 MPa, 10% AD: 5.36 ± 0.552 MPa). No significant decrease in compressive strength was observed with increased AD concentration. No cytotoxicity was observed for these AD concentrations when tested against rat mesenchymal stem cells. Changes in cement setting time, mechanical properties, microstructure, *in vitro* and *in vivo* release kinetics with increased concentration of methotrexate, an anticancer drug, incorporated into CPC was studied by Yang et al. [103] for local drug delivery application to address the local recurrence of bone tumors and systemic toxicities of chemotherapy. Methotrexate concentration of 0 wt.% (control), 0.2 wt.%, 0.5 wt.%, and 1 wt.% were mixed with CPC powder. The decrease in initial and final setting time with increase in drug concentration was statistically insignificant with respect to control. No statistically significant decrease in compressive and tensile strength was observed up to 0.5 wt.% drug concentration. Similar *in vitro* release kinetics were observed for all drug concentration up to 30 days. Although an increase in total drug release each day was observed with increased drug concentration into CPC matrix, total percentage release was decreased with increased concentration. CPC (with 1 wt.% methotrexate) containing 1.02 mg drug in each implant

was implanted into rabbit thigh muscle, and no side-effects on the gastrointestinal system and wound healing were observed. Release pattern similar to *in vitro* was also observed for *in vivo*.

Tanzawa et al. [190] showed that an anticancer drug, cisplatin, incorporated alone into CPC inhibited the bone tumor activity only for 4 weeks. Bone tumor forming cells regained their activity after 4 weeks. Incorporation of cisplatin and caffeine together showed a prolonged anti-tumor activity due to sustained release of caffeine, which inhibited further proliferation of tumor cells damaged by cisplatin. Caffeine was used as a cytocidal enhancer of the anticancer drug against bone and soft tissue tumors. Doadrio et al. [191] investigated cephalexin, an antibiotic, drug release behavior from a calcium sulphate (gypsum) cement and hydroxyapatite (HA)/calcium sulphate composite cement. Cephalexin content 1 wt.% was mixed into the solid phase of the cement. Approximately 80–90% of the drug was released after 8 h in SBF from calcium sulphate cement. More controlled release kinetics were observed, when HA was used with calcium sulphate. Only 25% of the drug was released after 8 h from HA/calcium sulphate composite cement, and 90% of the drug was released after one week. Incorporation of stem cells (SCs), such as human bone marrow-derived mesenchymal stem cells (hBMMSCs), into CPC has also been investigated [192] to induce increased mineralization through osteogenic differentiation of hBMMSCs. hBMMSCs were encapsulated into alginate beads by Weir and Xu [192], and subsequently mixed with either (i) a CPC (control), (ii) CPC reinforced with chitosan or (iii) CPC reinforced with chitosan plus degradable Vicryl fibers. The encapsulated cells in CPC–chitosan and CPC–chitosan–fiber remained viable greater than 70% on day 21. Encapsulated hBMMSCs under-went osteogenic differentiation by increased ALP activity and mineral deposition observed by scanning electron microscopy (SEM) and powder X-ray diffraction (XRD).

6.1. Limitations of CPC

Often, incorporation of drugs potentially deteriorates mechanical properties of CPC. Alkhraisat et al. [193] observed an increase in final setting time and decrease in tensile strength, when doxycycline hyclate (DOXY-h) (an antibiotic, commonly used in dentistry to defeat periodontal pathogens) was incorporated into CPC. Pelletier et al. [194] reported a decrease in compressive strength of CPC with an increased concentration of antibiotic drugs, flucloxacillin and vancomycin. Ratier et al. [195] also observed a decrease in compressive strength with an increase in tetracycline concentration, an antibiotic drug. A morphological change in the CPC with increases in tetracycline concentration was also reported. This is interpreted due to the strong affinity of tetracycline hydrochloride to CaP. Ratier et al. [195] addressed this limitation to some extent by treating tetracycline hydrochloride with CaP solution and then incorporating it into CPC. A maximum of 7% drug was incorporated without affecting the mechanical properties of CPC. Hesaraki et al. [186] also observed an increase in setting time and decrease in crystallinity of CPC by incorporating an antibiotic drug, cephalexin monohydrate. An increase in setting time was also reported by Bohner et al. [196] due to gentamicin sulphate incorporation into the CPC matrix. Drug release from CPC depends also on the intrinsic porosity, which is directly related to processing parameters [183,196]. Despite excellent osteoconductivity and ease of applicability, use of CPCs as drug delivery vehicles is limited. Limitations in the application are mostly due to the changes in the final properties of CPCs resulting from the drug incorporation, changes in the drug activity and its bioavailability.

6.2. CPC polymer composite

CPCs are by nature mechanically weak, and degrade more rapidly than the sintered CaP scaffolds. Polymers are usually added to CPC to increase the mechanical properties and

control degradation [197–199]. Increased setting time and reduced workability are also reported with increased mechanical properties [200–202]. Polymeric materials such as chitosan [203,204], alginate [205,206] and gelatin [207–209] have been used to improve the anti-washout and handling properties of CPCs as these materials tend to disintegrate on early contact with blood and other fluid. Bohner et al. [210] added poly(acrylic acid) (PAA) to control gentamicin sulphate (GS), an antibiotic, release from CPC for local drug delivery application. GS release was affected by the PAA-to-GS ratio present in the CPC matrix. At lower PAA/GS ratio (<0.7), up to 1– 2 days' release was observed with the square root of time release kinetics. At higher PAA/GS ratio (>0.7), a prolonged release (up to 8 days) was observed with a combination of square root of time and zero order release kinetics. The dependence of drug release kinetics on the interactions between drug and polymer, polymer molecular weight, and solubility of the polymer was observed. Ruhe et al. [211] studied rhBMP-2 release behavior from rhBMP-2 loaded PLGA/CaP cement. It was reported that the release of rhBMP-2 was dependent on the composite composition and nanostructure, as well as the pH of the release medium. Fullana et al. [212] investigated low-methoxy amidated pectins (LMAP) polysaccharide/CaP cement system to introduce macroporosity and controlled drug release using ibuprofen, a non-steroidal anti-inflammatory drug. Reduction in setting time and mechanical properties were observed in the presence of LMAP. The drug release rate was found to be dependent on the LMAP ratio with a sustained release for 45 days. Table 7 summarizes a list of some common drugs used in musculoskeletal disorders treatment that are mentioned in this review.

6.2.1. Concerns with CPC polymer composite—Niikura et al. [213], in a case study of a human patient with methicillin-resistant *S aureus* osteomyelitis, showed that vancomycin- impregnated polymethylmethacrylate (PMMA) beads were not as effective as vancomycin-impregnated BIOPEX, a CPC. The thermal heat generated during vancomycin-impregnated PMMA setting altered the drug activity, while the CPC did not. The deleterious effects of organic additives, delayed setting time and decreased mechanical strength are reported by Ginebra et al. [182]. It has also been shown that incorporation of alendronate into CPC delays the transformation rate of α-TCP to CDHA, and a decrease in mechanical strength of the CPC due to an increase in the drug concentration [214].

6.3. Release behavior from CPC

Drug release kinetics are influenced by physico-chemical properties such as solubility and chemical nature of the drug, microstructure, crystallinity, density, and porosity of the resulting CPC. Interaction between the drug and the cement, and the degradation behavior of CPCs, are also often affected by the changes during hydration and setting [176]. If a polymer is used in the CPC matrix, drug release kinetics also depend on its molecular weight, solubility, degradation rate, and drug–polymer interaction. In general, depending on the drug release behavior, drug delivery devices (DDDs) can be categorized into three major classes: diffusion controlled, chemical processes controlled, and externally or electronically controlled [215]. The degradation of drug incorporated CPC matrix is usually a slower process than the drug release kinetics. For this reason, drug release kinetics is generally a diffusion dominated process from the biodegradable CPCs. Degradation related release [216] is also a simultaneous process with this diffusion. Fig. 14c illustrates the schematic of drug release from a CPC loaded with drug molecules (red zig-zags).

Diffusion dominated release kinetics from a matrix can be described by the square root of time kinetics, the Higuchi law. The Higuchi law is based on Fickian diffusion under the assumption that drug molecules are uniformly dispersed in a homogeneous matrix. A simplistic form of the Higuchi equation is [193,216]:

$$M = k\sqrt{t}$$

where M is the cumulative percentage drug release at time t and k is the release rate constant that incorporates structural and geometric nature of the matrix.

In practical experimental conditions, drug release kinetics fit the Higuchi equation for shorter duration of release. For longer duration, release kinetics do not always follow the Higuchi law, because factors other than diffusion start influencing drug release kinetics after a certain time. Sometimes changes in cement matrix composition, such as increasing the polymer-to-CaP phase ratio, may also lead to dominate release kinetics other than the square root of time kinetics [210]. Hydrophobic–hydrophilic interactions between drug-polymer and drug-release medium also could influence the release kinetics, which might not follow simple power laws.

7. Concluding remarks and future directions

CaPs show excellent bioactivity and biocompatibility in the physiological conditions due to their chemical similarities to the inorganic part of bone, and they are non-immunogenic. CaPs have been used successfully in various drug delivery applications in the form of nanoscale (particulate systems) to microscale (coating) to macroscale (CPC and scaffold) for local delivery, and in some cases for targeted delivery. Although, the last decade has witnessed outstanding progresses in drug delivery approaches from different ceramic systems, many scientific and technological challenges still remain to be addressed. A better understanding of the microenvironment around the implant–host tissue interface will lead us to develop a drug delivery system to treat musculoskeletal disorders more effectively. Cell signaling through integrin protein family, present at the cell membrane, recruits the specific integrin receptors to communicate with the extracellular matrix (ECM) molecules. Next generation drug delivery systems will be required to trigger need-based functions at the cellular microenvironment through recruiting and generating ECM molecules for specific functions. Recent advances in CaP-based drug delivery systems discussed here present the application versatility of CaPs as drug or bone growth factor delivery vehicles to treat various musculoskeletal disorders and diseases. Future developments in this area would require paying attention to the challenges and issues that have been highlighted in this review. Efficacy and efficiency of the on-site and targeted drug delivery from CaP systems need to be optimized with reproducibility. Not only the release kinetics and CaP–drug interactions, but also the physicochemical properties of different CaP delivery systems, need to be understood and optimized. We believe that new and improved approaches to address the existing limitations will open up new avenues for applicability of CaP drug delivery systems in the near future. Successful approaches need to exert more precise control at micro- and nanoscale levels along with integrated knowledge capturing the fundamentals of multiple disciplines such as chemistry, biology, engineering and in-depth animal studies to develop CaP-based drug delivery systems.

Acknowledgments

The authors would like to thank the National Institute of Health, NIBIB for financial support (Grant # NIH-R01-EB-007351).

References

1. National Osteoporosis Foundation. Available from: http://www.nof.org

2. Kim S. Changes in surgical loads and economic burden of hip and knee replacements in the US: 1997–2004. Arthritis Rheum. 2008; 59(4):481–8. [PubMed: 18383407]
3. American Academy Of Orthopaedic Surgeons (AAOS). Available from: http://orthoinfo.aaos.org
4. United States Bone and Joint Initiative. Available from: http://www.usbjd.org
5. Bose S, Tarafder S, Edgington J, Bandyopadhyay A. Calcium phosphate ceramics in drug delivery. JOM. 2011; 63:93–8.
6. Groot, KD. Bioceramics of calcium phosphate. Boca Raton, FL: CRC Press; 1983.
7. LeGeros RZ. Calcium phosphate-based osteoinductive materials. Chem Rev. 2008; 108:4742–53. [PubMed: 19006399]
8. Rey C. Calcium phosphate biomaterials and bone mineral. Differences in composition, structures and properties. Biomaterials. 1990; 11:13–5. [PubMed: 2397252]
9. Ratner, BD.; Hoffman, AS.; Schoen, FJ.; Lemons, JE. Biomaterials science: an introduction to materials in medicine. 2. New York: Academic Press; 2004.
10. Bandyopadhyay A, Bernard S, Xue W, Bose S. Calcium phosphate-based resorbable ceramics: influence of MgO, ZnO, and SiO_2 dopants. J Am Cer Soc. 2006; 89:2675–88.
11. Dorozhkin SV, Epple M. Biological and medical significance of calcium phosphates. Angew Chem Int Ed. 2002; 41:3130–46.
12. Bourne, GH.; Herring, GM. The organic matrix of bone. The biochemistry and physiology of bone. New York: Academic Press; 1972. p. 127-89.
13. Porter JR, Ruckh TT, Popat KC. Bone tissue engineering: a review in bone biomimetics and drug delivery strategies. Biotechnol Prog. 2009; 25:1539–60. [PubMed: 19824042]
14. Palmer LC, Newcomb CJ, Kaltz SR, Spoerke ED, Stupp SI. Biomimetic systems for hydroxyapatite mineralization inspired by bone and enamel. Chem Rev. 2008; 108:4754–83. [PubMed: 19006400]
15. LeGeros RZ. Properties of osteoconductive biomaterials: calcium phosphates. Clin Orthop Relat Res. 2002; 395:81–98. [PubMed: 11937868]
16. Liu Y, de Groot K, Hunziker E. BMP-2 liberated from biomimetic implant coatings induces and sustains direct ossification in an ectopic rat model. Bone. 2005; 36:745–57. [PubMed: 15814303]
17. Blom EJ, Klein-Nulend J, Wolke JGC, van Waas MAJ, Driessens FCM, Burger EH. Transforming growth factor-β1 incorporation in a calcium phosphate bone cement: material properties and release characteristics. J Biomed Mater Res. 2002; 59:265–72. [PubMed: 11745562]
18. Weir MD, Xu HH. High-strength, in situ-setting calcium phosphate composite with protein release. J Biomed Mater Res. 2008; 85A:388–96.
19. Ikawa N, Kimura T, Oumi Y, Sano T. Amino acid containing amorphous calcium phosphates and the rapid transformation into apatite. J Mater Chem. 2009; 19:4906–13.
20. Takahashi T, Tominaga T, Watabe N, Yokobori AT, Sasada H, Yoshimoto T. Use of porous hydroxyapatite graft containing recombinant human bone morphogenetic protein-2 for cervical fusion in a caprine model. J Neurosurgery: Spine. 1999; 90:224–30.
21. Yoshida K, Bessho K, Fujimura K, Konishi Y, Kusumoto K, Ogawa Y, et al. Enhancement by recombinant human bone morphogenetic protein-2 of bone formation by means of porous hydroxyapatite in mandibular bone defects. J Dent Res. 1999; 78:1505–10. [PubMed: 10512384]
22. Bohner M, Lemaitre J. Can bioactivity be tested *in vitro* with SBF solution? Biomaterials. 2009; 30:2175–9. [PubMed: 19176246]
23. Pietrzak, WS. Musculoskeletal tissue regeneration: biological materials and methods. New Jersey: Humana Press; 2008. p. 161-2.
24. Bohner M. Calcium orthophosphates in medicine: from ceramics to calcium phosphate cementsortofosfatos de calcio en medicina: de la cerámica a los cementos de fosfato de calcio. Injury. 2000; 31(Suppl 4):D37–47.
25. Lai C, Tang S, Wang Y, Wei K. Formation of calcium phosphate nanoparticles in reverse microemulsions. Mater Lett. 2005; 59:210–4.
26. Roy I, Mitra S, Maitra A, Mozumdar S. Calcium phosphate nanoparticles as novel non-viral vectors for targeted gene delivery. Int J Pharm. 2003; 250:25–33. [PubMed: 12480270]

27. Maitra A. Calcium phosphate nanoparticles: second-generation nonviral vectors in gene therapy. Expert Rev Mol Diagn. 2005; 5:893–905. [PubMed: 16255631]
28. Li Y, Weng W, Tam KC. Novel highly biodegradable biphasic tricalcium phosphates composed of [alpha]-tricalcium phosphate and [beta]-tricalcium phosphate. Acta Biomater. 2007; 3:251–4. [PubMed: 16979393]
29. Matsushita N, Terai H, Okada T, Nozaki K, Inoue H, Miyamoto S, et al. A new bone-inducing biodegradable porous β-tricalcium phosphate. J Biomed Mater Res. 2004; 70A:450–8.
30. Nery EB, LeGeros RZ, Lynch KL, Lee K. Tissue response to biphasic calcium phosphate ceramic with different ratios of HA/beta TCP in periodontal osseous defects. J Periodontol. 1992; 63:729–35. [PubMed: 1335498]
31. Arinzeh TL, Tran T, Mcalary J, Daculsi G. A comparative study of biphasic calcium phosphate ceramics for human mesenchymal stem-cell-induced bone formation. Biomaterials. 2005; 26:3631–8. [PubMed: 15621253]
32. Kannan S, Lemos I, Rocha J, Ferreira J. Synthesis and characterization of magnesium substituted biphasic mixtures of controlled hydroxyapatite/[beta]-tricalcium phosphate ratios. J Solid State Chem. 2005; 178:3190–6.
33. Fernandez E, Gil FJ, Ginebra MP, Driessens FCM, Planell JA, Best SM. Calcium phosphate bone cements for clinical applications. Part I. Solution chemistry. J Mater Sci: Mater Med. 1999; 10:169–76. [PubMed: 15348165]
34. Habraken W, Wolke J, Jansen J. Ceramic composites as matrices and scaffolds for drug delivery in tissue engineering. Adv Drug Delivery Rev. 2007; 59:234–48.
35. Lin X, Samia A. Synthesis, assembly and physical properties of magnetic nanoparticles. J Magn Magn Mater. 2006; 305:100–9.
36. Chen X, Wang B, Shi C, Zhang. Hydrothermal synthesis and self-assembly of magnetite (Fe_3O_4) nanoparticles with the magnetic and electrochemical properties. J Crystal Growth. 2008; 310:5453–7.
37. Lee J, et al. Artificially engineered magnetic nanoparticles for ultra-sensitive molecular imaging. Nat Med. 2007; 13(1):95–9. [PubMed: 17187073]
38. Trewyn BG, Slowing II, Giri S, Chen H, Lin VS. Synthesis and functionalization of a mesoporous silica nanoparticle based on the sol–gel process and applications in controlled release. Acc Chem Res. 2007; 40:846–53. [PubMed: 17645305]
39. Yang W, Zhang CG, Qu HY, Yang HH, Xu JG. Novel fluorescent silica nanoparticle probe for ultrasensitive immunoassays. Anal Chim Acta. 2004; 503:163–9.
40. Gemeinhart RA, Luo D, Saltzman WM. Cellular fate of a modular DNA delivery system mediated by silica nanoparticles. Biotechnol Prog. 2008; 21:532–7. [PubMed: 15801794]
41. Tsoli M, Kuhn H, Brandau W, Esche H, Schmid G. Cellular uptake and toxicity of Au55 clusters. Small. 2005; 1:841–4. [PubMed: 17193536]
42. Paciotti GF, Kingston DG, Tamarkin L. Colloidal gold nanoparticles: a novel nanoparticle platform for developing multifunctional tumor-targeted drug delivery vectors. Drug Dev Res. 2006; 67:47–54.
43. Pissuwan D, Valenzuela SM, Cortie MB. Therapeutic possibilities of plasmonically heated gold nanoparticles. Trends Biotechnol. 2006; 24:62–7. [PubMed: 16380179]
44. Zhu X, et al. A facile method for preparation of gold nanoparticles with high SERS efficiency in the presence of inositol hexaphosphate. J Colloid Interface Sci. 2010; 342:571–4. [PubMed: 19932487]
45. Fu H, Hu Y, McNelis T, Hollinger JO. A calcium phosphate-based gene delivery system. J Biomed Mater Res A. 2005; 74:40–8. [PubMed: 15920737]
46. Cheng X, Kuhn L. Chemotherapy drug delivery from calcium phosphate nanoparticles. Int J Nanomed. 2007; 2:667–74.
47. Liu T, Tang A, Zhang G, Chen Y, Zhang J, Peng S, et al. Calcium phosphate nanoparticles as a novel nonviral vector for efficient transfection of DNA in cancer gene therapy. Cancer Biother Radiopharm. 2005; 20:141–9. [PubMed: 15869447]

48. Chu T, He Q, Potter DE. Biodegradable calcium phosphate nanoparticles as a new vehicle for delivery of a potential ocular hypotensive agent. J Ocul Pharmacol Ther. 2002; 18:507–14. [PubMed: 12537677]
49. Chowdhury E, Kunou M, Nagaoka M, Kundu A, Hoshiba T, Akaike T. High-efficiency gene delivery for expression in mammalian cells by nanoprecipitates of Ca–Mg phosphate. Gene. 2004; 341:77–82. [PubMed: 15474290]
50. Adair JH, Parette MP, Altınoğlu EI, Kester M. Nanoparticulate alternatives for drug delivery. ACS Nano. 2010; 4:4967–70. [PubMed: 20873786]
51. Tan W, Wang K, He X, Zhao XJ, Drake T, Wang L, et al. Bionanotechnology based on silica nanoparticles. Med Res Rev. 2004; 24:621–38. [PubMed: 15224383]
52. Yao G, Wang L, Wu Y, Smith J, Xu J, Zhao W, et al. FloDots: luminescent nanoparticles. Anal Bioanal Chem. 2006; 385:518–24. [PubMed: 16715275]
53. Manuel C, Foster M, Monteiro F, Ferraz M, Doremus RH, Bizios R. Preparation and characterization of calcium phosphate nanoparticles. Key Eng Mater. 2004; 254–256:903–6.
54. Manuel C, Ferraz M, Monteiro F. Synthesis of hydroxyapatite and tricalcium phosphate nanoparticles – preliminary studies. Key Eng Mater. 2003; 240–242:555–8.
55. Zyman ZZ, Rokhmistrov DV, Glushko VI. Structural and compositional features of amorphous calcium phosphate at the early stage of precipitation. J Mater Sci: Mater Med. 2009:21123–30.
56. Araujo T, Souza S, Miyakawa W, Sousa M. Phosphates nanoparticles doped with zinc and manganese for sunscreens. Mater Chem Phys. 2010; 124:1071–6.
57. Bose S, Saha SK. Synthesis of hydroxyapatite nanopowders via sucrose-templated sol–gel method. J Am Cer Soc. 2003; 86:1055–7.
58. Hanifi A, Fathi MH, Mir Mohammad Sadeghi H, Varshosaz J. Mg^{2+} substituted calcium phosphate nano particles synthesis for non viral gene delivery application. J Mater Sci: Mater Med. 2010; 21:2393–401. [PubMed: 20464457]
59. Abu Osman NA, Ibrahim F, Wan Abas WAB, Abdul Rahman HS, Ting H. 4th Kuala Lumpur International Conference on Biomedical Engineering. IFMBE Proceedings. 2008; 21(3):314–317.
60. Jahandideh R, Behnamghader A, Rangie M, Youzbashi A, Joughehdoust S, Tolouei R. Sol–gel synthesis of FHA nanoparticles and CDHA agglomerates from a mixture with a nonstochiometric Ca/P ratio. Key Eng Mater. 2009; 396–398:607–10.
61. Loher S, et al. Fluoro-apatite and calcium phosphate nanoparticles by flame synthesis. Chem Mater. 2005; 17:36–42.
62. Suchanek WL, Byrappa K, Shuk P, Riman RE, Janas VF, TenHuisen KS. Mechanochemical–hydrothermal synthesis of calcium phosphate powders with coupled magnesium and carbonate substitution. J Solid State Chem. 2004; 177:793–9.
63. Sun L, Chow LC, Frukhtbeyn SA, Bonevich JE. Preparation and properties of nanoparticles of calcium phosphates with various Ca/P ratios. J Res Natl Inst Stand Technol. 2010; 115:243–55. [PubMed: 21037948]
64. Wu Y, Bose S. Nanocrystalline hydroxyapatite: micelle templated synthesis and characterization. Langmuir. 2005; 21:3232–4. [PubMed: 15807558]
65. Bose S, Saha SK. Synthesis and characterization of hydroxyapatite nanopowders by emulsion technique. Chem Mater. 2003; 15:4464–9.
66. Banerjee A, Bandyopadhyay A, Bose S. Hydroxyapatite nanopowders: synthesis, densification and cell–materials interaction. Mater Sci Eng: C. 2007; 27:729–35.
67. Dasgupta S, Bandyopadhyay A, Bose S. Reverse micelle-mediated synthesis of calcium phosphate nanocarriers for controlled release of bovine serum albumin. Acta Biomater. 2009; 5:3112–21. [PubMed: 19435617]
68. Shum HC, Bandyopadhyay A, Bose S, Weitz DA. Double emulsion droplets as microreactors for synthesis of mesoporous hydroxyapatite. Chem Mater. 2009; 21:5548–55.
69. Wang S, McDonnell EH, Sedor FA, Toffaletti JG. PH effects on measurements of ionized calcium and ionized magnesium in blood. Arch Pathol Lab Med. 2002; 126:947–50. [PubMed: 12171493]
70. Tycko B, Maxfield FR. Rapid acidification of endocytic vesicles containing alpha 2-macroglobulin. Cell. 1982; 28:643–51. [PubMed: 6176331]

71. Epple M, Kovtun A. Functionalized calcium phosphate nanoparticles for biomedical application. Key Eng Mater. 2010; 441:299–305.
72. Stubbs M, McSheehy PM, Griffiths JR, Bashford CL. Causes and consequences of tumour acidity and implications for treatment. Mol Med Today. 2000; 6:15–9. [PubMed: 10637570]
73. Cheung H, Lau K, Lu T, Hui D. A critical review on polymer-based bio-engineered materials for scaffold development. Compos Part B: Eng. 2007; 38:291–300.
74. Habraken WJ, Zhang Z, Wolke JG, Grijpma DW, Mikos AG, Feijen J, et al. Introduction of enzymatically degradable poly(trimethylene carbonate) microspheres into an injectable calcium phosphate cement. Biomaterials. 2008; 29:2464–76. [PubMed: 18328556]
75. Kester M, et al. Calcium phosphate nanocomposite particles for *in vitro* imaging and encapsulated chemotherapeutic drug delivery to cancer cells. Nano Lett. 2008; 8:4116–21. [PubMed: 19367878]
76. Morgan TT, et al. Encapsulation of organic molecules in calcium phosphate nanocomposite particles for intracellular imaging and drug delivery. Nano Lett. 2008; 8:4108–15. [PubMed: 19367837]
77. Pouton CW, Seymour LW. Key issues in non-viral gene delivery. Adv Drug Delivery Rev. 1998; 34:3–19.
78. Xu ZP, Zeng QH, Lu GQ, Yu AB. Inorganic nanoparticles as carriers for efficient cellular delivery. Chem Eng Sci. 2006; 61:1027–40.
79. Reischl D, Zimmer A. Drug delivery of siRNA therapeutics: potentials and limits of nanosystems. Nanomedicine: Nanotechnol Biol Med. 2009; 5:8–20.
80. Partridge KA, Oreffo RO. Gene delivery in bone tissue engineering: progress and prospects using viral and nonviral strategies. Tissue Eng. 2004; 10:295–307. [PubMed: 15009954]
81. Olton D, Li J, Wilson ME, Rogers T, Close J, Huang L, et al. Nanostructured calcium phosphates (NanoCaPs) for non-viral gene delivery: influence of the synthesis parameters on transfection efficiency. Biomaterials. 2007; 28:1267–79. [PubMed: 17123600]
82. Kumta PN, Sfeir C, Lee D, Olton D, Choi D. Nanostructured calcium phosphates for biomedical applications: novel synthesis and characterization. Acta Biomater. 2005; 1:65–83. [PubMed: 16701781]
83. Chen W, Lin M, Lin P, Tasi P, Chang Y, Yamamoto S. Studies of the interaction mechanism between single strand and double-strand DNA with hydroxyapatite by microcalorimetry and isotherm measurements. Colloids Surf A: Physicochem Eng Aspects. 2007; 295:274–83.
84. Sokolova V, Epple M. Inorganic nanoparticles as carriers of nucleic acids into cells. Angew Chem Int Ed. 2008; 47:1382–95.
85. Zhang G, Liu T, Chen Y, Chen Y, Xu M, Peng J, et al. Tissue specific cytotoxicity of colon cancer cells mediated by nanoparticle-delivered suicide gene *in vitro* and *in vivo*. Clin Cancer Res. 2009; 15:201–7. [PubMed: 19118047]
86. Mondéjar SP, Kovtun A, Epple M. Lanthanide-doped calcium phosphate nanoparticles with high internal crystallinity and with a shell of DNA as fluorescent probes in cell experiments. J Mater Chem. 2007; 17:4153–9.
87. Neumeier M, Hails LA, Davis SA, Mann S, Epple M. Synthesis of fluorescent core–shell hydroxyapatite nanoparticles. J Mater Chem. 2011; 21:1250–4.
88. Lebugle A, Pellé F, Charvillat C, Rousselot I, Chane-Ching J. Colloidal and monocrystalline Ln3 doped apatite calcium phosphate as biocompatible fluorescent probes. Chem Commun. 2006; 6:606–8.
89. He X, Wang K, Cheng Z. *In vivo* near-infrared fluorescence imaging of cancer with nanoparticle-based probes. WIREs Nanomed Nanobiotechnol. 2010; 2:349–66.
90. Muddana HS, Morgan TT, Adair JH, Butler PJ. Photophysics of Cy3-encapsulated calcium phosphate nanoparticles. Nano Lett. 2009; 9:1559–66. [PubMed: 19260707]
91. Ganesan K, Kovtun A, Neumann S, Heumann R, Epple M. Calcium phosphate nanoparticles: colloidally stabilized and made fluorescent by a phosphate-functionalized porphyrin. J Mater Chem. 2008; 18:3655.
92. Banerjee SS, Roy M, Bose S. PH Tunable fluorescent calcium phosphate nanocomposite for sensing and controlled drug delivery. Adv Eng Mater. 2010:B10–7.

93. Altınoğlu EI, et al. Near-infrared emitting fluorophore-doped calcium phosphate nanoparticles for *in vivo* imaging of human breast cancer. ACS Nano. 2008; 2:2075–84. [PubMed: 19206454]
94. Dasgupta S, Banerjee SS, Bandyopadhyay A, Bose S. Zn- and Mg-doped hydroxyapatite nanoparticles for controlled release of protein. Langmuir. 2010; 26:4958–64. [PubMed: 20131882]
95. Sokolova VV, Radtke I, Heumann R, Epple M. Effective transfection of cells with multi-shell calcium phosphate-DNA nanoparticles. Biomaterials. 2006; 27:3147–53. [PubMed: 16469375]
96. Lew PDP, Waldvogel PFA. Osteomyelitis. The Lancet. 2004; 364:369–79.
97. Schäfer P, Fink B, Sandow D, Margull A, Berger I, Frommelt L. Prolonged bacterial culture to identify late periprosthetic joint infection: a promising strategy. Clin Infec Dis. 2008; 47:1403–9. [PubMed: 18937579]
98. Frommelt L. Principles of systemic antimicrobial therapy in foreign material associated infection in bone tissue, with special focus on periprosthetic infection. Injury. 2006; 37:S87–94. [PubMed: 16651077]
99. Ewald A, Hösel D, Patel S, Grover LM, Barralet JE, Gbureck U. Silver-doped calcium phosphate cements with antimicrobial activity. Acta Biomater. 2011; 7:4064–70. [PubMed: 21763795]
100. Acharya G, Park K. Mechanisms of controlled drug release from drug-eluting stents. Adv Drug Delivery Rev. 2006; 58:387–401.
101. Wang PP, Frazier J, Brem H. Local drug delivery to the brain. Adv Drug Delivery Rev. 2002; 54:987–1013.
102. Radin S, Campbell JT, Ducheyne P, Cuckler JM. Calcium phosphate ceramic coatings as carriers of vancomycin. Biomaterials. 1997; 18:777–82. [PubMed: 9177855]
103. Yang Z, Li D, Han J, Li J, Li X, Li Z, et al. Incorporation of methotrexate in calcium phosphate cement: behavior and release *in vitro* and *in vivo*. Orthopedics. 2009; 32:27. [PubMed: 19226038]
104. Ip M, Lui SL, Poon VKM, Lung I, Burd A. Antimicrobial activities of silver dressings: an *in vitro* comparison. J Med Microbiol. 2006; 55:59–63. [PubMed: 16388031]
105. Pratten J, Nazhat SN, Blaker JJ, Boccaccini AR. *In vitro* attachment of *Staphylococcus epidermidis* to surgical sutures with and without Ag-containing bioactive glass coating. J Biomater Appl. 2004; 19:47–57. [PubMed: 15245643]
106. Roy M, Bandyopadhyay A, Bose S. *In vitro* antimicrobial and biological properties of laser assisted tricalcium phosphate coating on titanium for load bearing implant. Mater Sci Eng: C. 2009; 29:1965–8.
107. Kokubo T, Takadama H. How useful is SBF in predicting *in vivo* bone bioactivity? Biomaterials. 2006; 27:2907–15. [PubMed: 16448693]
108. Liu Y, Wu G, de Groot K. Biomimetic coatings for bone tissue engineering of critical-sized defects. J R Soc Interface. 201010.1098/rsif.2010.0115.focus
109. Stigter M, Bezemer J, de Groot K, Layrolle P. Incorporation of different antibiotics into carbonated hydroxyapatite coatings on titanium implants, release and antibiotic efficacy. J Control Release. 2004; 99:127–37. [PubMed: 15342186]
110. Barrere F, van Blitterswijk CA, de Groot K, Layrolle P. Influence of ionic strength and carbonate on the Ca–P coating formation from SBF × 5 solution. Biomaterials. 2002; 23:1921–30. [PubMed: 11996032]
111. Habibovic P, Barrère F, Blitterswijk CA, Groot K, Layrolle P. Biomimetic hydroxyapatite coating on metal implants. J Am Ceram Soc. 2004; 85:517–22.
112. Rogers MJ, Gordon S, Benford HL, Coxon FP, Luckman SP, Monkkonen J, et al. Cellular and molecular mechanisms of action of bisphosphonates. Cancer. 2000; 88:2961–78. [PubMed: 10898340]
113. Roelofs AJ, Thompson K, Gordon S, Rogers MJ. Molecular mechanisms of action of bisphosphonates: current status. Clin Cancer Res. 2006; 12:6222s–30s. [PubMed: 17062705]
114. Van Beek E, Löwik C, Van Der Pluijm G, Papapoulos S. The role of geranylgeranylation in bone resorption and its suppression by bisphosphonates in fetal bone explants *in vitro*: a clue to the mechanism of action of nitrogen-containing bisphosphonates. J Bone Miner Res. 1999; 14:722–9. [PubMed: 10320520]

115. Ezra A, Golomb G. Administration routes and delivery systems of bisphosphonates for the treatment of bone resorption. Adv Drug Delivery Rev. 2000; 42:175–95.

116. Peter B, et al. Calcium phosphate drug delivery system: influence of local zoledronate release on bone implant osteointegration. Bone. 2005; 36:52–60. [PubMed: 15664002]

117. Garbuz DS, et al. Enhanced gap filling and osteoconduction associated with alendronate–calcium phosphate-coated porous tantalum. J Bone Joint Surg Am. 2008; 90:1090–100. [PubMed: 18451402]

118. Li T, Lee J, Kobayashi T, Aoki H. Hydroxyapatite coating by dipping method, and bone bonding strength. J Mater Sci: Mater Med. 1996; 7:355–7.

119. Kim H, Koh Y, Li L, Lee S, Kim H. Hydroxyapatite coating on titanium substrate with titania buffer layer processed by sol–gel method. Biomaterials. 2004; 25:2533–8. [PubMed: 14751738]

120. Hirai S, Nishinaka K, Shimakage K, Uo M, Watari F. Hydroxyapatite coating on titanium substrate by the sol–gel process. J Am Ceram Soc. 2004; 87:29–34.

121. Albayrak O, El-Atwani O, Altintas S. Hydroxyapatite coating on titanium substrate by electrophoretic deposition method: effects of titanium dioxide inner layer on adhesion strength and hydroxyapatite decomposition. Surf Coat Technol. 2008; 202:2482–7.

122. Wei M, Ruys AJ, Swain MV, Kim SH, Milthorpe BK, Sorrell CC. Interfacial bond strength of electrophoretically deposited hydroxyapatite coatings on metals. J Mater Sci Mater Med. 1999; 10:401–9. [PubMed: 15348125]

123. Campbell AA, Fryxell GE, Linehan JC, Graff GL. Surface-induced mineralization: a new method for producing calcium phosphate coatings. J Biomed Mater Res. 1996; 32:111–8. [PubMed: 8864879]

124. Hamdi M, Hakamata S, Ektessabi AM. Coating of hydroxyapatite thin film by simultaneous vapor deposition. Thin Solid Films. 2000; 377–378:484–9.

125. Saju, KK.; Reshmi, R.; Jayadas, NH.; James, J.; Jayaraj, MK. Polycrystalline coating of hydroxyapatite on TiAl6V4 implant material grown at lower substrate temperatures by hydrothermal annealing after pulsed laser deposition. J Eng Med; Proceedings of the Institution of Mechanical Engineers, Part H; 2009. p. 1049-57.

126. Roy M, Vamsi Krishna B, Bandyopadhyay A, Bose S. Laser processing of bioactive tricalcium phosphate coating on titanium for load-bearing implants. Acta Biomater. 2008; 4:324–33. [PubMed: 18039597]

127. Roy M, Bandyopadhyay A, Bose S. Laser surface modification of electrophoretically deposited hydroxyapatite coating on titanium. J Am Ceram Soc. 2008; 91:3517–21.

128. Roy M, Bandyopadhyay A, Bose S. Induction plasma sprayed nano hydroxyapatite coatings on titanium for orthopaedic and dental implants. Surf Coat Technol. 2011; 205:2785–92. [PubMed: 21552358]

129. Esenwein SA, Esenwein S, Herr G, Muhr G, Küsswetter W, Hartwig CH. Osteogenetic activity of BMP-3-coated titanium specimens of different surface texture at the orthotopic implant bed of giant rabbits. Chirurg. 2001; 72:1360–8. [PubMed: 11766662]

130. Karageorgiou V, Kaplan D. Porosity of 3D biomaterial scaffolds and osteogenesis. Biomaterials. 2005; 26:5474–91. [PubMed: 15860204]

131. Ramay HRR, Zhang M. Biphasic calcium phosphate nanocomposite porous scaffolds for load-bearing bone tissue engineering. Biomaterials. 2004; 25:5171–80. [PubMed: 15109841]

132. Bose S, Suguira S, Bandyopadhyay A. Processing of controlled porosity ceramic structures via fused deposition. Scr Mater. 1999; 41:1009–14.

133. Yang S, Leong K, Du Z, Chua C. The design of scaffolds for use in tissue engineering. Part I. Traditional factors. Tissue Eng. 2001; 7:679–89. [PubMed: 11749726]

134. Boontheekul T, Mooney DJ. Protein-based signaling systems in tissue engineering. Curr Opin Biotechnol. 2003; 14:559–65. [PubMed: 14580589]

135. Kempen DH, Creemers LB, Alblas J, Lu L, Verbout AJ, Yaszemski MJ, et al. Growth factor interactions in bone regeneration. Tissue Eng Part B: Rev. 2010; 16:551–66. [PubMed: 21039299]

136. Kofron MD, Laurencin CT. Bone tissue engineering by gene delivery. Adv Drug Deliv Rev. 2006; 58:555–76. [PubMed: 16790291]

137. Kassem M, Blum W, Ristelli J, Mosekilde L, Eriksen EF. Growth hormone stimulates proliferation and differentiation of normal human osteoblast-like cells *in vitro*. Calcif Tissue Int. 1993; 52:222–6. [PubMed: 7683248]
138. Ohlsson C, Bengtsson B, Isaksson OGP, Andreassen TT, Slootweg MC. Growth hormone and bone. Endocrine Rev. 1998; 19:55–79. [PubMed: 9494780]
139. Guicheux J, et al. Human growth hormone locally released in bone sites by calcium–phosphate biomaterial stimulates ceramic bone substitution without systemic effects: a rabbit study. J Bone Miner Res. 1998; 13:739–48. [PubMed: 9556073]
140. Sengupta S, Gherardi E, Sellers LA, Wood JM, Sasisekharan R, Fan TD. Hepatocyte growth factor/scatter factor can induce angiogenesis independently of vascular endothelial growth factor. ATVB. 2003; 23:69–75.
141. Zambonin G, Camerino C, Greco G, Patella V, Moretti B, Grano M. Hydroxyapatite coated with hepatocyte growth factor (HGF) stimulates human osteoblasts *in vitro*. J Bone Joint Surg Br. 2000; 82-B(3):457–60. [PubMed: 10813189]
142. Hossain M, Irwin R, Baumann M, McCabe L. Hepatocyte growth factor (HGF) adsorption kinetics and enhancement of osteoblast differentiation on hydroxyapatite surfaces. Biomaterials. 2005; 26:2595–602. [PubMed: 15585262]
143. Koempel JA, Patt BS, O'Grady K, Wozney J, Toriumi DM. The effect of recombinant human bone morphogenetic protein-2 on the integration of porous hydroxyapatite implants with bone. J Biomed Mater Res. 1998; 41:359–63. [PubMed: 9659603]
144. Dellinger JG, Eurell JAC, Jamison RD. Bone response to 3D periodic hydroxyapatite scaffolds with and without tailored microporosity to deliver bone morphogenetic protein 2. J Biomed Mater Res. 2006; 76A:366–76.
145. Lan Levengood SK, et al. The effect of BMP-2 on micro- and macroscale osteointegration of biphasic calcium phosphate scaffolds with multiscale porosity. Acta Biomater. 2010; 6:3283–91. [PubMed: 20176148]
146. Woodard JR, et al. The mechanical properties and osteoconductivity of hydroxyapatite bone scaffolds with multi-scale porosity. Biomaterials. 2007; 28:45–54. [PubMed: 16963118]
147. Polak SJ, Levengood SKL, Wheeler MB, Maki AJ, Clark SG, Johnson AJW. Analysis of the roles of microporosity and BMP-2 on multiple measures of bone regeneration and healing in calcium phosphate scaffolds. Acta Biomater. 2011; 7:1760–71. [PubMed: 21199692]
148. Deans RJ, Moseley AB. Mesenchymal stem cells: biology and potential clinical uses. Exp Hematol. 2000; 28:875–84. [PubMed: 10989188]
149. Bianco P, Riminucci M, Gronthos S, Robey PG. Bone marrow stromal stem cells: nature, biology, and potential applications. Stem cells. 2001; 19:180–92. [PubMed: 11359943]
150. Martin I, Muraglia A, Campanile G, Cancedda R, Quarto R. Fibroblast growth factor-2 supports ex vivo expansion and maintenance of osteogenic precursors from human bone marrow. Endocrinol. 1997; 138:4456–62.
151. Roldán J, et al. Bone formationanddegradationofa highlyporous biphasic calcium phosphate ceramic inpresence ofBMP-7, VEGF andmesenchymal stemcells inan ectopic mouse model. J Cranio-Maxillofac Sur. 2010; 38:423–30.
152. Kundu B, et al. Development of new localized drug delivery system based on ceftriaxone-sulbactam composite drug impregnated porous hydroxyapatite: a systematic approach for *in vitro* and *in vivo* animal trial. Pharm Res. 2010; 27:1659–76. [PubMed: 20464462]
153. Xue W, Bandyopadhyay A, Bose S. Polycaprolactone coated porous tricalcium phosphate scaffolds for controlled release of protein for tissue engineering. J Biomed Mater Res Part B: Appl Biomater. 2009; 91:831–8. [PubMed: 19572301]
154. Rai B, Teoh S, Hutmacher D, Cao T, Ho K. Novel PCL-based honeycomb scaffolds as drug delivery systems for rhBMP-2. Biomaterials. 2005; 26:3739–48. [PubMed: 15621264]
155. Ghasemi-Mobarakeh L, Prabhakaran MP, Morshed M, Nasr-Esfahani MH, Ramakrishna S. Bio-functionalized PCL nanofibrous scaffolds for nerve tissue engineering. Mater Sci Eng: C. 2010; 30:1129–36.

156. Mattanavee W, Suwantong O, Puthong S, Bunaprasert T, Hoven VP, Supaphol P. Immobilization of biomolecules on the surface of electrospun polycaprolactone fibrous scaffolds for tissue engineering. ACS Appl Mater Interfaces. 2009; 1:1076–85. [PubMed: 20355894]
157. Kim HW, Knowles JC, Kim HE. Hydroxyapatite/poly(-caprolactone) composite coatings on hydroxyapatite porous bone scaffold for drug delivery. Biomaterials. 2004; 25:1279–87. [PubMed: 14643602]
158. Kuboki Y, et al. BMP-Induced osteogenesis on the surface of hydroxyapatite with geometrically feasible and nonfeasible structures: topology of osteogenesis. J Biomed Mater Res. 1998; 39:190–9. [PubMed: 9457547]
159. Hui PW, Leung PC, Sher A. Fluid conductance of cancellous bone graft as a predictor for graft–host interface healing. J Biomech. 1996; 29:123–32. [PubMed: 8839025]
160. Kuboki Y, Jin Q, Takita H. Geometry of carriers controlling phenotypic expression in BMP-induced osteogenesis and chondrogenesis. J Bone Joint Surg Am. 2001; 83:S105–115. [PubMed: 11314788]
161. Doblaré M, García JM, Gómez MJ. Modelling bone tissue fracture and healing: a review. Eng Fracture Mech. 2004; 71:1809–40.
162. Hutmacher DW. Scaffolds in tissue engineering bone and cartilage. Biomaterials. 2000; 21:2529–43. [PubMed: 11071603]
163. Liu C, Xia Z, Czernuszka J. Design and development of three-dimensional scaffolds for tissue engineering. Chem Eng Res Des. 2007; 85:1051–64.
164. Zein I, Hutmacher DW, Tan KC, Teoh SH. Fused deposition modeling of novel scaffold architectures for tissue engineering applications. Biomaterials. 2002; 23:1169–85. [PubMed: 11791921]
165. Sachlos E, Czernuszka J. Making tissue engineering scaffolds work. Eur Cells Mater. 2003; 5:29–40.
166. Butscher A, Bohner M, Hofmann S, Gauckler L, Müller R. Structural and material approaches to bone tissue engineering in powder-based three-dimensional printing. Acta Biomater. 2011; 7:907–20. [PubMed: 20920616]
167. Will J, Melcher R, Treul C, Travitzky N, Kneser U, Polykandriotis E, et al. Porous ceramic bone scaffolds for vascularized bone tissue regeneration. J Mater Sci: Mater Med. 2008; 19:2781–90. [PubMed: 18305907]
168. Hollister SJ. Porous scaffold design for tissue engineering. Nat Mater. 2005; 4:518–24. [PubMed: 16003400]
169. Vail NK, Swain LD, Fox WC, Aufdlemorte TB, Lee G, Barlow JW. Materials for biomedical applications. Mater Des. 1999; 20:123–32.
170. Sun W, Starly B, Darling A, Gomez C. Computer-aided tissue engineering: application to biomimetic modelling and design of tissue scaffolds. Biotechnol Appl Biochem. 2004; 39:49–58. [PubMed: 14556653]
171. Kalita SJ, Bose S, Hosick HL, Bandyopadhyay A. Development of controlled porosity polymer–ceramic composite scaffolds via fused deposition modeling. Mater Sci Eng: C. 2003; 23:611–20.
172. Bandyopadhyay A, Das K, Marusich J, Onagoruwa S. Application of fused deposition in controlled microstructure metal–ceramic composites. Rapid Prototyping J. 2006; 12:121–8.
173. Roussière H, et al. Reaction of zoledronate with β-tricalcium phosphate for the design of potential drug device combined systems. Chem Mater. 2008; 20:182–91.
174. Legeros R, Chohayeb A, Shulman A. Apatitic calcium phosphates: possible dental restorative materials. J Dent Res. 1982; 61:343–7.
175. Brown WE, Chow LC. A new calcium phosphate setting cement. J Den Res. 1983; 62:672.
176. Ginebra M, Traykova T, Planell J. Calcium phosphate cements as bone drug delivery systems: a review. J Control Release. 2006; 113:102–10. [PubMed: 16740332]
177. Bohner M. Reactivity of calcium phosphate cements. J Mater Chem. 2007; 17:3980–6.
178. Bohner M, Brunner TJ, Stark WJ. Controlling the reactivity of calcium phosphate cements. J Mater Chem. 2008; 18:5669–75.

179. Brunner TJ, Grass RN, Bohner M, Stark WJ. Effect of particle size, crystal phase and crystallinity on the reactivity of tricalcium phosphate cements for bone reconstruction. J Mater Chem. 2007; 17:4072–8.
180. Fernandez E, Boltong M, Ginebra M, Driessens F, Bermudez O, Planell J. Development of a method to measure the period of swelling of calcium phosphate cements. J Mater Sci Lett. 1996; 15:1004–5.
181. Ginebra M, Driessens F, Planell J. Effect of the particle size on the micro and nanostructural features of a calcium phosphate cement: a kinetic analysis. Biomaterials. 2004; 25:3453–62. [PubMed: 15020119]
182. Ginebra MP, Boltong MG, Fernandez E, Planell JA, Driessens FCM. Effect of various additives and temperature on some properties of an apatitic calcium phosphate cement. J Mater Sci: Mater Med. 1995; 6:612–6.
183. Espanol M, Perez R, Montufar E, Marichal C, Sacco A, Ginebra M. Intrinsic porosity of calcium phosphate cements and its significance for drug delivery and tissue engineering applications. Acta Biomater. 2009; 5:2752–62. [PubMed: 19357005]
184. Yu T, Ye J, Gao C, Yu L, Wang Y. Synthesis and drug delivery property of calcium phosphate cement with special crystal morphology. J Am Ceram Soc. 2010; 93:1241–4.
185. Stallmann HP, Faber C, Bronckers AL, Amerongen N, Arie V, Wuisman PI. In vitro gentamicin release from commercially available calcium-phosphate bone substitutes influence of carrier type on duration of the release profile. BMC Musculoskeletal Disorders. 2006; 7:18. [PubMed: 16504140]
186. Hesaraki S, Nemati R. Cephalexin-loaded injectable macroporous calcium phosphate bone cement. J Biomed Mater Res. 2009; 89B:342–52.
187. Stallmann HP, Roo RD, Faber C, Amerongen AVN, Wuisman PI. *In vivo* release of the antimicrobial peptide hLF1-11 from calcium phosphate cement. J Orthop Res. 2008; 26:531–8. [PubMed: 17972323]
188. Stallmann HP. Osteomyelitis prevention in rabbits using antimicrobial peptide hLF1-11- or gentamicin-containing calcium phosphate cement. J Antimicrob Chemother. 2004; 54:472–6. [PubMed: 15231767]
189. Jindong Z, Hai T, Junchao G, Bo W, Li B, Qiang WB. Evaluation of a novel osteoporotic drug delivery system in vitro: alendronate-loaded calcium phosphate cement. Orthopedics. 2010; 33:561.
190. Tanzawa Y, et al. Potentiation of the antitumor effect of calcium phosphate cement containing anticancer drug and caffeine on rat osteosarcoma. J Orthop Sci. 2011; 16:77–84. [PubMed: 21360005]
191. Doadrio JC, Arcos D, Cabañas MV, Vallet-Regí M. Calcium sulphate-based cements containing cephalexin. Biomaterials. 2004; 25:2629–35. [PubMed: 14751749]
192. Weir MD, Xu HH. Human bone marrow stem cell-encapsulating calcium phosphate scaffolds for bone repair. Acta Biomater. 2010; 6:4118–26. [PubMed: 20451676]
193. Alkhraisat MH, et al. Loading and release of doxycycline hyclate from strontium-substituted calcium phosphate cement. Acta Biomater. 2010; 6:1522–8. [PubMed: 19879982]
194. Pelletier MH, Malisano L, Smitham PJ, Okamoto K, Walsh WR. The compressive properties of bone cements containing large doses of antibiotics. J Arthroplasty. 2009; 24:454–60. [PubMed: 18534462]
195. Ratier A, Gibson I, Best S, Freche M, Lacout J, Rodriguez F. Setting characteristics and mechanical behaviour of a calcium phosphate bone cement containing tetracycline. Biomaterials. 2001; 22:897–901. [PubMed: 11311008]
196. Bohner M, Lemaitre J, Landuyt PV, Zambelli P, Merkle HP, Gander B. Gentamicin-loaded hydraulic calcium phosphate bone cement as antibiotic delivery system. J Pharm Sci. 1997; 86:565–72. [PubMed: 9145380]
197. Durucan C, Brown PW. Calcium-deficient hydroxyapatite-PLGA composites: mechanical and microstructural investigation. J Biomed Mater Res. 2000; 51:726–34. [PubMed: 10880122]
198. Durucan C, Brown PW. Low temperature formation of calcium-deficient hydroxyapatite–PLA/PLGA composites. J Biomed Mater Res. 2000; 51:717–25. [PubMed: 10880121]

199. Fujishiro Y, Takahashi K, Sato T. Preparation and compressive strength of alpha-tricalcium phosphate/gelatin gel composite cement. J Biomed Mater Res. 2001; 54:525–30. [PubMed: 11426597]
200. Miyazaki K, Horibe T, Antonucci JM, Takagi S, Chow LC. Polymeric calcium phosphate cements: analysis of reaction products and properties. Dent Mater. 1993; 9:41–5. [PubMed: 8299869]
201. Miyazaki K, Horibe T, Antonucci JM, Takagi S, Chow LC. Polymeric calcium phosphate cements: setting reaction modifiers. Dent Mater. 1993; 9:46–50. [PubMed: 8299870]
202. dos Santos LA, De Oliveria LC, Rigo EC, Carrodeguas RG, Boschi AO, De Arruda AC. Influence of polymeric additives on the mechanical properties of alpha-tricalcium phosphate cement. Bone. 1999; 25:99S–102S. [PubMed: 10458286]
203. Zhang Y, Zhang M. Calcium phosphate/chitosan composite scaffolds for controlled in vitro antibiotic drug release. J Biomed Mater Res. 2002; 62:378–86. [PubMed: 12209923]
204. Zhang Y, Xu HH. Effects of synergistic reinforcement and absorbable fiber strength on hydroxyapatite bone cement. J Biomed Mater Res. 2005; 75A:832–40.
205. Tajima S, Nishimoto N, Kishi Y, Matsuya S, Ishikawa K. Effects of added sodium alginate on mechanical strength of apatite cement. Dent Mater J. 2004; 23:329–34. [PubMed: 15510861]
206. Ishikawa K, Miyamoto Y, Takechi M, Toh T, Kon M, Nagayama M, et al. Non-decay type fast-setting calcium phosphate cement: hydroxyapatite putty containing an increased amount of sodium alginate. J Biomed Mater Res. 1997; 36:393–9. [PubMed: 9260110]
207. Bigi A, Bracci B, Panzavolta S. Effect of added gelatin on the properties of calcium phosphate cement. Biomaterials. 2004; 25:2893–9. [PubMed: 14962568]
208. Chiang T, Ho C, Chen DC, Lai M, Ding S. Physicochemical properties and biocompatibility of chitosan oligosaccharide/gelatin/calcium phosphate hybrid cements. Mater Chem Phys. 2010; 120:282–8.
209. Shie M, Chen DC, Wang C, Chiang T, Ding S. Immersion behavior of gelatin-containing calcium phosphate cement. Acta Biomater. 2008; 4:646–55. [PubMed: 18083642]
210. Bohner M, Lemaitre J, Merkle HP, Gander B. Control of gentamicin release from a calcium phosphate cement by admixed poly(acrylic acid). J Pharm Sci. 2000; 89:1262–70. [PubMed: 10980501]
211. Ruhe PQ, Hedberg EL, Padron NT, Spauwen PH, Jansen JA, Mikos AG. RhBMP-2 release from injectable poly(DL-lactic-co-glycolic acid)/calcium–phosphate cement composites. J Bone Joint Surg Am. 2003; 85:75–81. [PubMed: 12925613]
212. Girod Fullana S, Ternet H, Freche M, Lacout J, Rodriguez F. Controlled release properties and final macroporosity of a pectin microspheres-calcium phosphate composite bone cement. Acta Biomater. 2010; 6:2294–300. [PubMed: 19931655]
213. Niikura T, Tsujimoto K, Yoshiya S, Tadokoro K, Kurosaka M, Shiba R. Vancomycin-impregnated calcium phosphate cement for methicill-inresistant *Staphylococcus aureus* femoral osteomyelitis. Orthopedics. 2007; 30:320. [PubMed: 17424700]
214. Panzavolta S, Torricelli P, Bracci B, Fini M, Bigi A. Functionalization of biomimetic calcium phosphate bone cements with alendronate. J Inorg Biochem. 2010; 104:1099–106. [PubMed: 20638728]
215. Ginebra M, Traykova T, Planell JA. Calcium phosphate cements: competitive drug carriers for the musculoskeletal system? Biomaterials. 2006; 27:2171–7. [PubMed: 16332349]
216. Gbureck U, Vorndran E, Barralet JE. Modeling vancomycin release kinetics from microporous calcium phosphate ceramics comparing static and dynamic immersion conditions. Acta Biomater. 2008; 4:1480–6. [PubMed: 18485844]

Appendix A. Figures with essential colour discrimination

Certain figures in this article, particularly Figures 1–4, 6, 8, 11– 15 and 17 are difficult to interpret in black and white. The full colour images can be found in the on-line version, at doi:10.1016/j.actbio.2011.11.017.

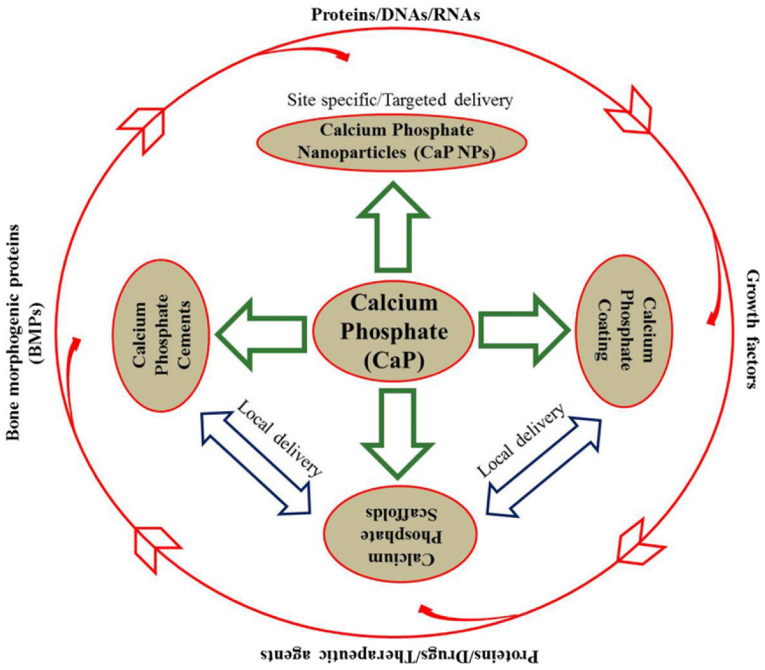

Fig. 1.
Application approaches of calcium phosphates in drug delivery and biomolecule.

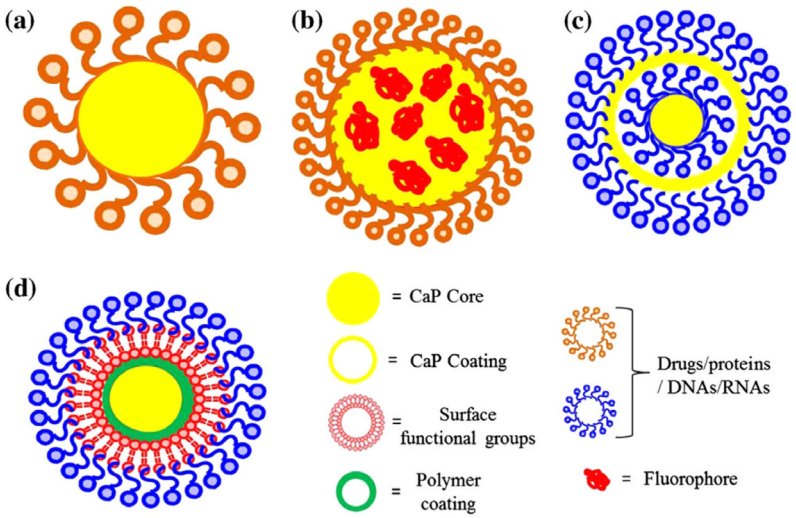

Fig. 2.

Schematic of CaP NPs for drug delivery applications: single shell (a and b), multi-shell (c), and surface functionalization approach (d). Fluorophore agents can be entrapped/doped into CaP core as shown in (b) for imaging. The multi-shell approach (c) is more effective for nuclear transfection than the single shell as in (a). Drugs or biomolecules that are poorly adsorbed on CaP can also be adsorbed on the surface functionalized polymer coating as shown in (d).

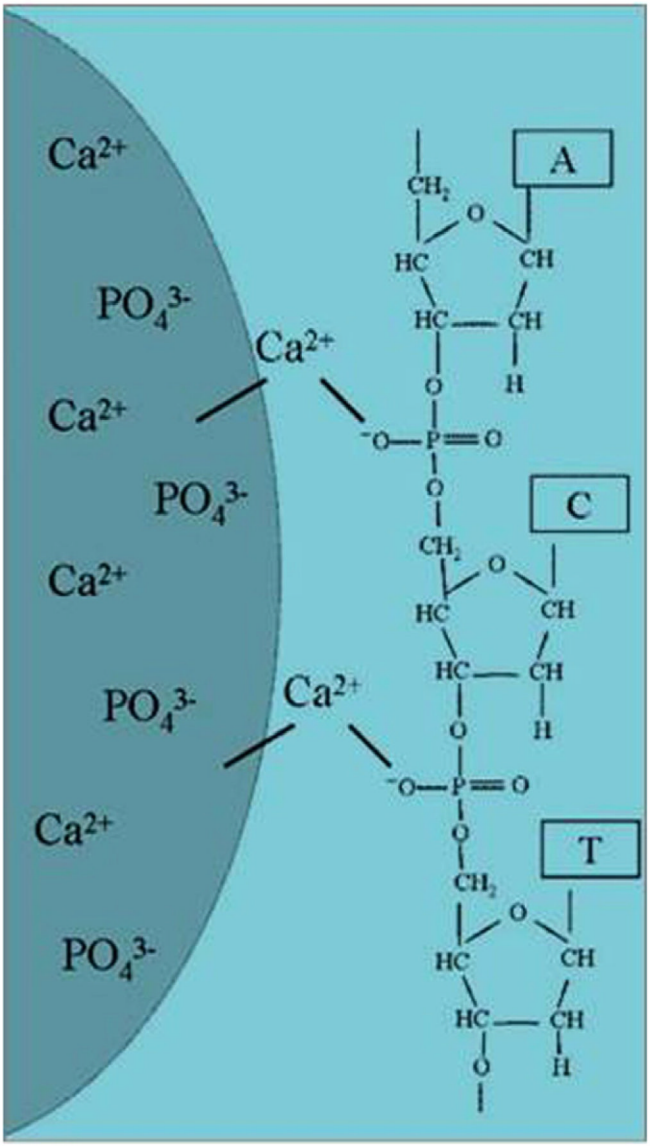

Fig. 3.
Schematic of the interaction of a nucleic acid on the CaP NP surface (Copyright (2008) Wiley-VCH Verlag GmbH & Co. KGaA. Reprinted from Ref. [84] with permission).

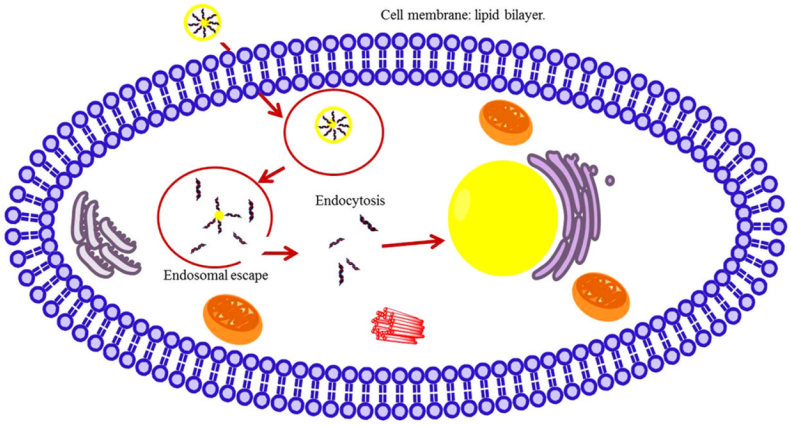

Fig. 4.
Schematic of transfection/intracellular delivery of drugs and biomolecules by CaP particles.

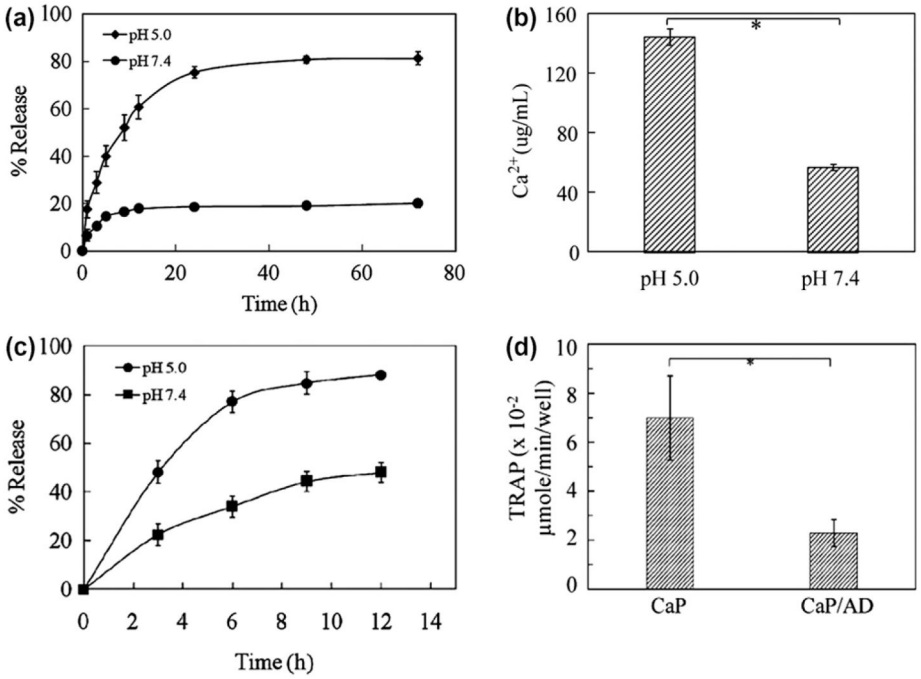

Fig. 5.

(a) Release profiles of AD from CaP/AD nanocomposite in PBS of pH 5.0 and pH 7.4; (b) dissolution of Ca^{2+} from CaP/AD nanocomposite after 72 h ($^{*}P < 0.05$); (c) release profiles of RDB from RDB-CaP/AD nanocomposite at different pH; (d) TRAP activity of osteoclast cells after 28 days of culture showing a threefold decrease in TRAP expression by CaP/AD nanocomposite compared to bare CaP nanoparticles ($P < 0.05$) (Copyright (2011) John Wiley and Sons Inc. Reprinted from Ref. [92] with permission).

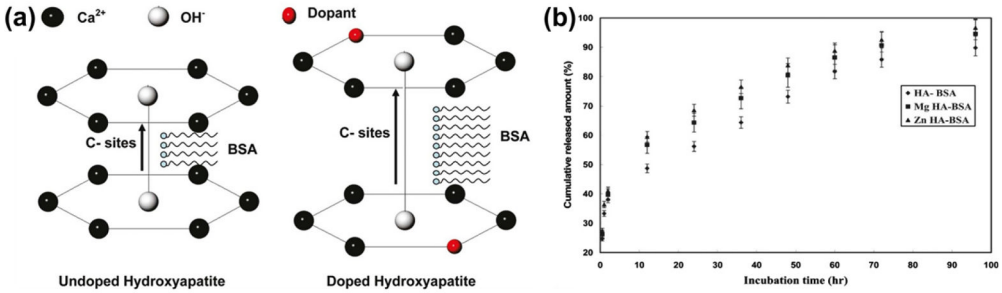

Fig. 6.

(a) Schematic showing the interaction between HA and BSA. Lengthening of the c-site of doped HA crystal lattice facilitated increased in situ BSA loading, (b) BSA release profile from the BSA loaded undoped (HA-BSA), magnesium-doped HA (Mg-HA-BSA), and zinc-doped HA (Zn-HA-BSA) nanoparticles (Copyright (2010) American Chemical Society. Reprinted from Ref. [94] with permission).

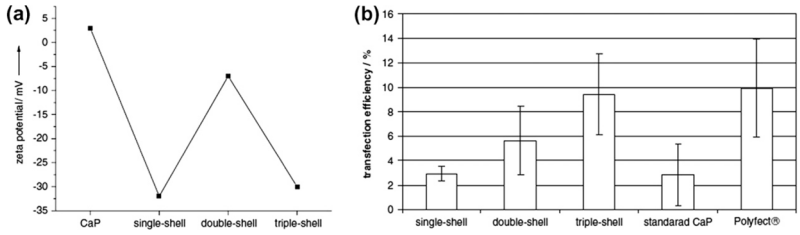

Fig. 7.

(a) Dependence of the zeta potential on the type of nanoparticles, demonstrating the addition of the differently charged outer layers (single shell and triple shell: DNA; double-shell: calcium phosphate); (b) comparison of the transfection efficiency of T-HUVEC in quantums medium by different methods. The error bars represent the standard deviation ($N = 3$). There were significant differences between single shell and triple shell ($P < 0.01$) and triple shell and the standard calcium phosphate method ($P < 0.05$) (Copyright (2006) Elsevier. Reprinted from Ref. [95] with permission).

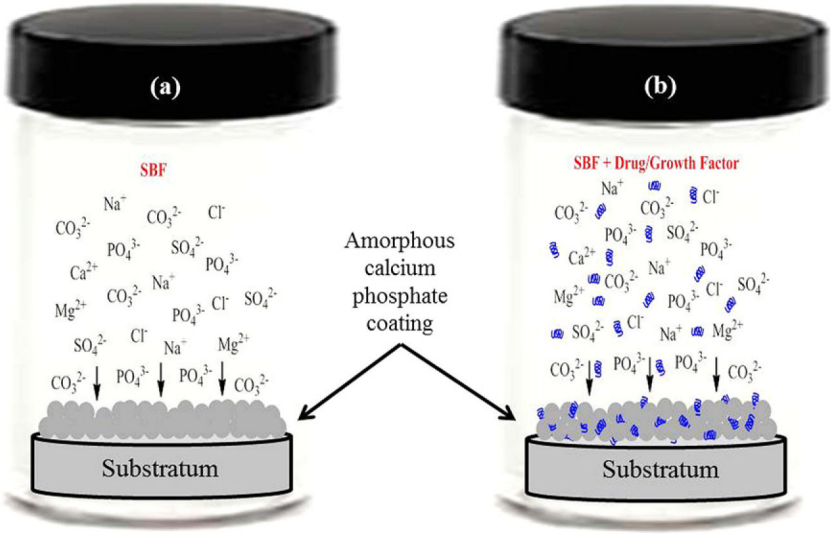

Fig. 8.

Schematic of biomimetic coating: (a) simple biomimetic coating of an amorphous calcium deficient carbonated apatite from SBF (usually the SBF ion concentration for biomimetic coating is 5 to 10 times higher than the normal SBF ion concentration); (b) biomimetic co-precipitation of drug/growth factor.

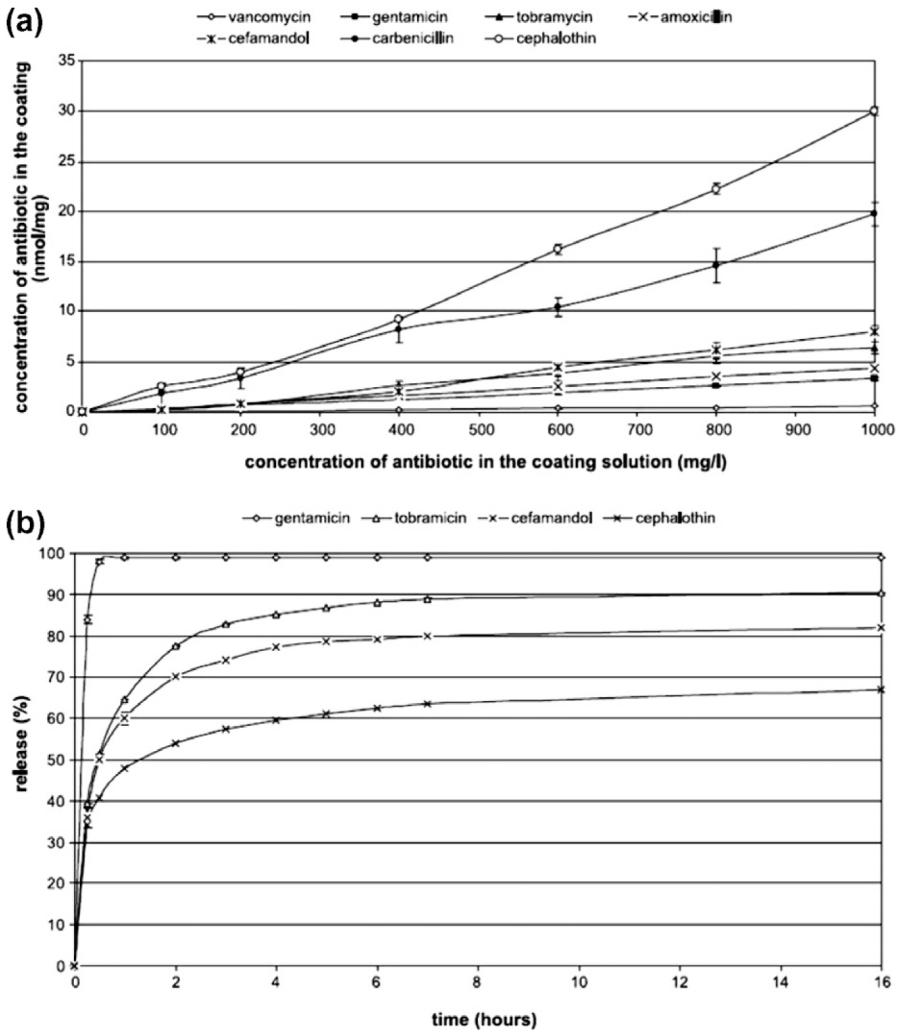

Fig. 9.

(a) Incorporation of antibiotic into the carbonated hydroxyapatite coating vs. the concentration in coating solution, (b) antibiotic release from carbonated hydroxyapatite coatings into PBS pH 7.3 (Copyright (2004) Elsevier. Reprinted from Ref. [109] with permission).

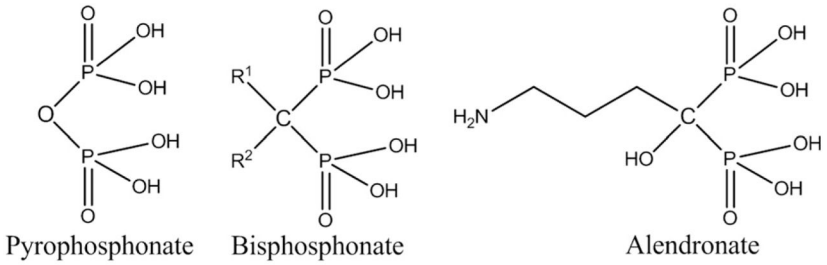

Fig. 10.

Structural similarities between inorganic pyrophosphate and bisphosphonates. Substitution of different functional groups at R^1 and R^2 positions generates a family of bisphosphonate drugs, here only showing alendronate.

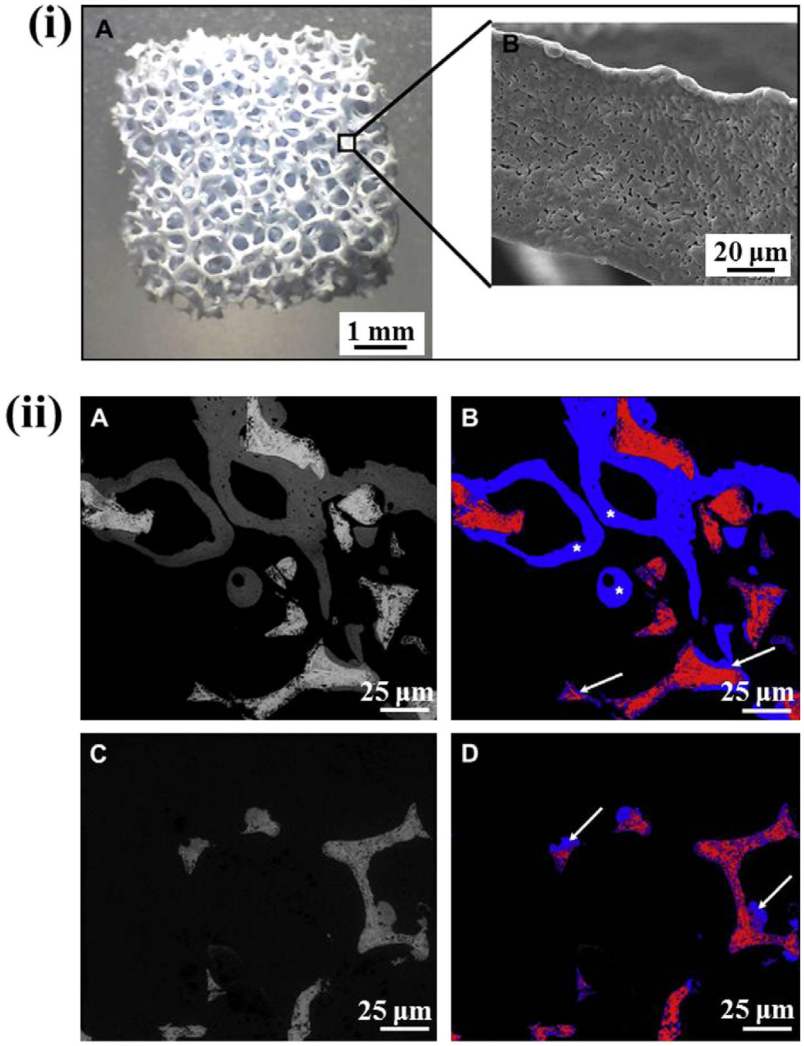

Fig. 11.

(i) Porous BCP scaffolds with 92–94% volume fraction porosity, and interconnected macropore size 360–440 μm and 900–1150 μm (A), and 0.4–4 μm micropore size in the strut (B); (ii) ESEM (environmental scanning electron microscopy) images of explanted BCP scaffolds stimulated with BMP-7 (A), and corresponding segmented image for the detection of newly formed bone (B). The grey values are assigned to different colors (ceramic: red, new bone: blue) and the area ratio of ceramic/new bone was calculated. New bone formation observed both at the surface (white arrows) and inside the pores (white stars) (B). A control BCP scaffold without any additives is presented in (C), with the corresponding image used for histomorphometric analysis (D) (Copyright (2010) Elsevier. Reprinted from Ref. [151] with permission).

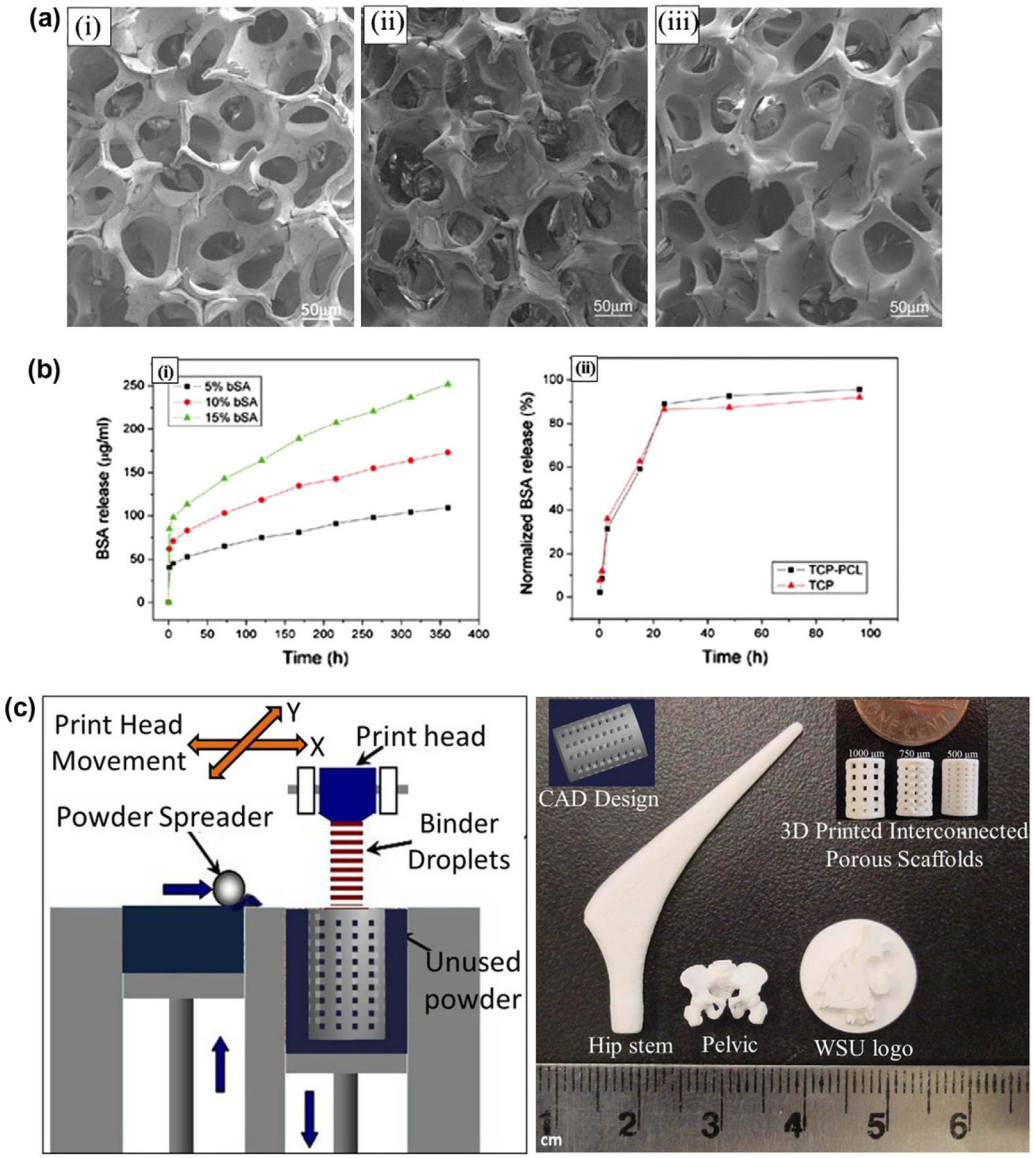

Fig. 12.

(a) SEM morphologies of the scaffolds: (i) TCP, (ii) TCP coated with 2.5% PCL w/v in dichloromethane, (iii) TCP coated with 5.0% PCL w/v in dichloromethane; (b) release profile of BSA: (i) from BSA incorporated into PCL-coated samples, (ii) from superficially BSA adsorbed samples. BSA incorporation into polymer (PCL) coating showed a relatively controlled release than the superficially adsorbed BSA samples (Copyright (2009) John Wiley and Sons. Reprinted from the reference. [153] with permission); (c) Schematic of 3D printing and some 3D printed parts (fabricated at Washington State University) showing the versatility of 3D printing technology for ceramic scaffolds fabrication with complex architectural features.

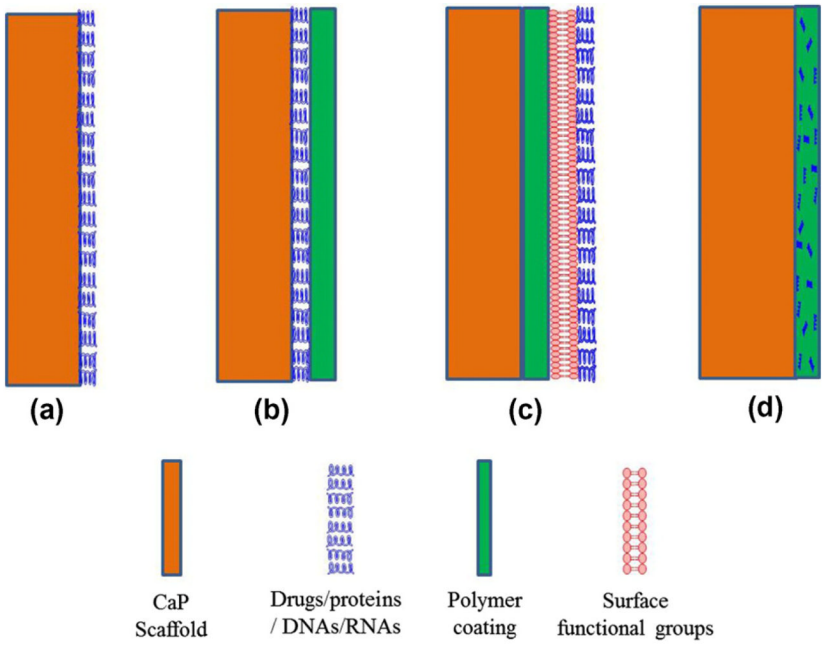

Fig. 13.

Schematic representation of drug loading approaches on CaP scaffolds: (a) adsorption on bare CaP scaffold; (b) adsorption of drugs on bare CaP scaffolds followed by polymer coating to prevent burst release and have a sustained release; (c) polymer coating on bare CaP scaffolds followed by surface treatment of the coating, then adsorption of drugs or conjugation of drug molecules by chemical treatment; and (d) drugs can be encapsulated into the polymer coating itself.

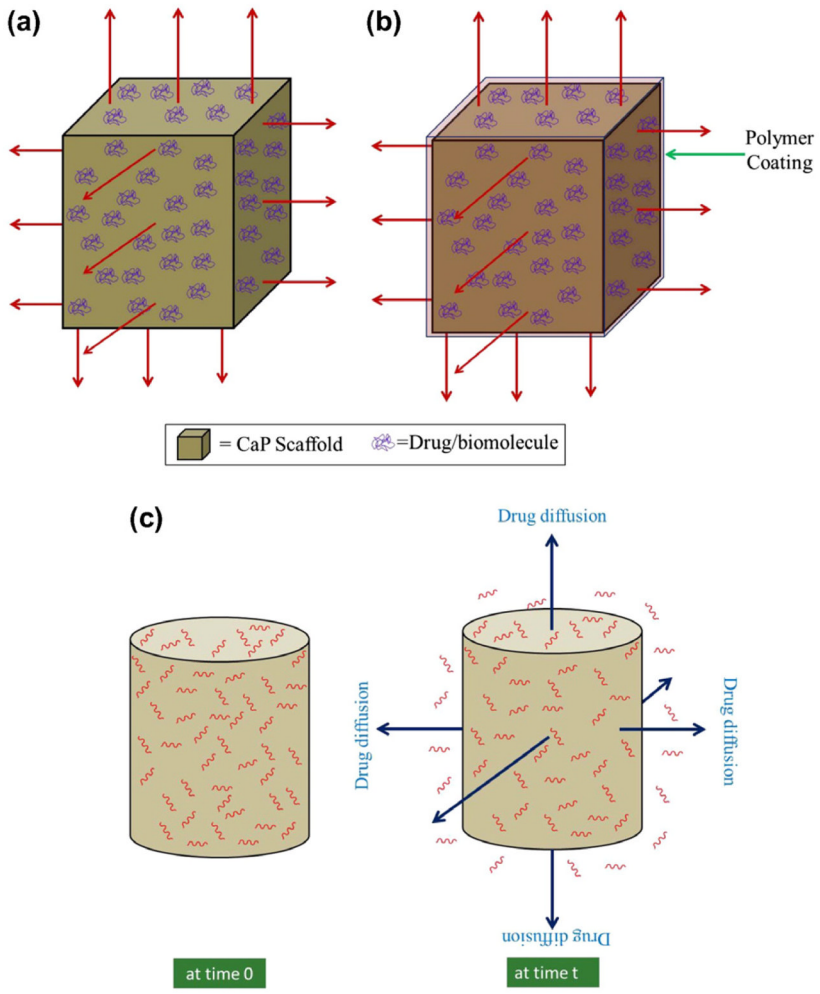

Fig. 14.

Schematic of drug release: from uncoated (a), and polymer-coated (b) CaP scaffolds, and a CPC loaded with drug molecules (red zig-zags) (c); blue arrows indicate the drug release.

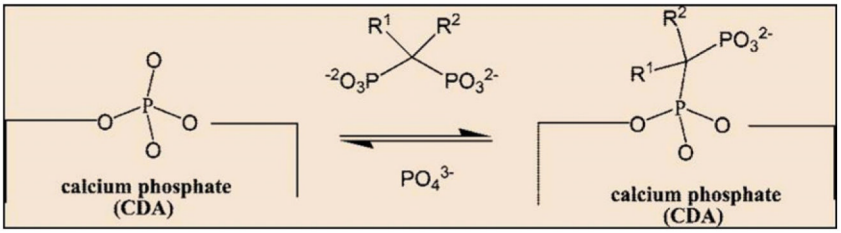

Fig. 15.
Schematic representation of the chemical association of bisphosphonates onto the surface of CDA particles, via a reversible BP for phosphate exchange (Copyright (2008) American Chemical Society. Reprinted from Ref. [173] with permission).

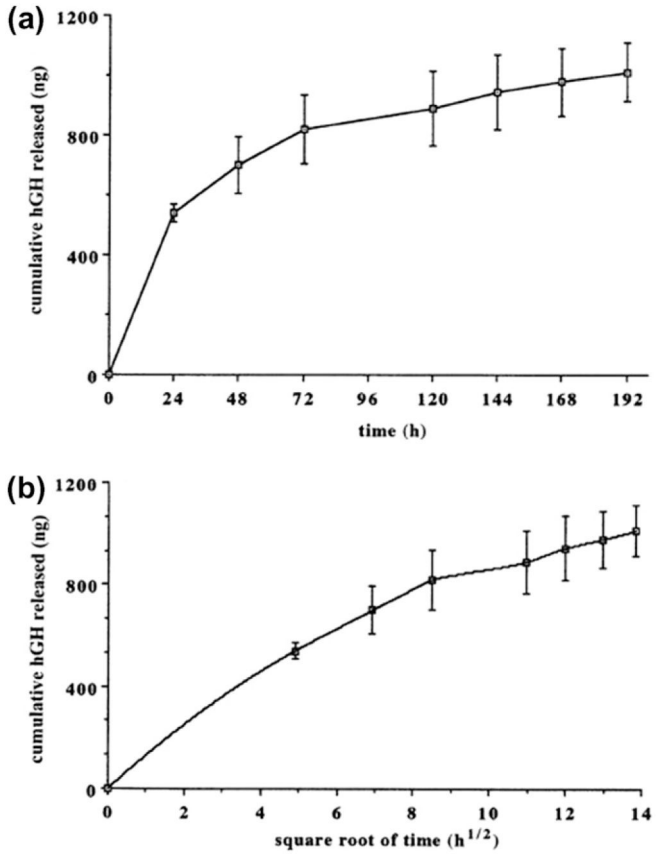

Fig. 16.

In vitro release profile of human growth hormone (hGH) from macroporous biphasic calcium phosphate (MBCP) ceramic: (a) cumulated hGH amount released; (b) Higuchi plot of the hGH release profile; ($n = 3$) (Copyright (1998) John Wiley and Sons. Reprinted from Ref. [139] with permission).

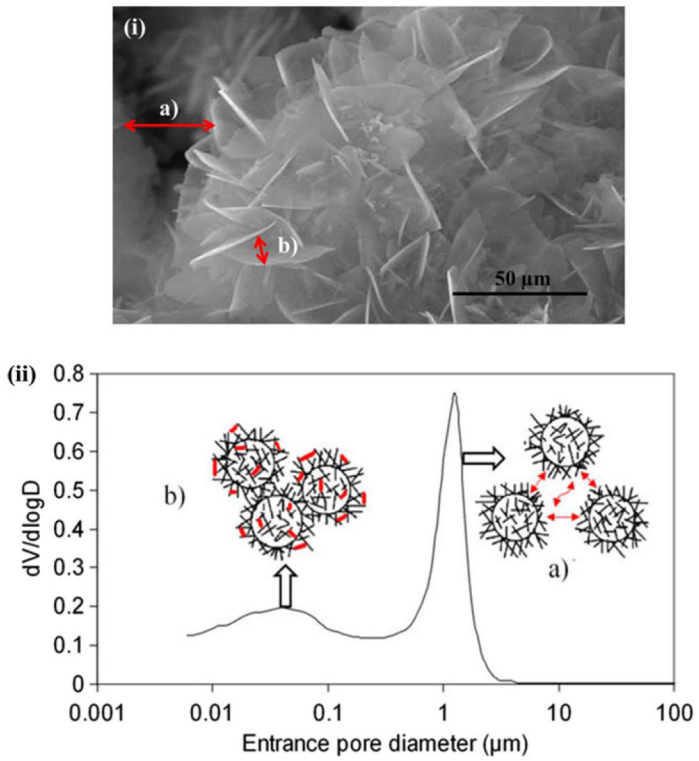

Fig. 17.

Two different types of pore distribution in a α-TCP cement measured by mercury intrusion porosimetry, and also observed in SEM image. Porosity between aggregates (a), and porosity between crystallites. These intrinsic porosities play a key role in drug adsorption and release (Copyright (2009) Elsevier. Reprinted from Ref. [183] with permission).

Table 1

Typical compositional values of inorganic phase of adult human calcified tissues (Copyright (2002) John Wiley and Sons. Reprinted from Ref. [11] with permission).

Composition	Enamel	Dentin	Bone	Hydroxyapatite (HA)
Calcium [wt.%]	36.5	35.1	34.8	39.6
Phosphorus (as P) [wt.%]	17.7	16.9	15.2	18.5
Ca/P (molar ratio)	1.63	1.61	1.71	1.67
Sodium [wt.%]	0.5	0.6	0.9	–
Magnesium [wt.%]	0.44	1.23	0.72	–
Potassium [wt.%]	0.08	0.05	0.03	–
Carbonate (as CO_3^{2-}) [wt.%]	3.5	5.6	7.4	–
Fluoride [wt.%]	0.01	0.06	0.03	–
Chloride [wt.%]	0.30	0.01	0.13	–
Pyrophosphate,(as $P_2O_7^{-4}$) [wt.%]	0.022	0.10	0.07	–
Total inorganic [wt.%]	97	70	65	100
Total organic [wt.%]	1.5	20	25	–
Water [wt.%]	1.5	10	10	–
Ignition products (800 °C)	β-TCP + HA	β-TCP + HA	HA + CaO	HA

Table 2

Organic component of bone and their functions in bone mineralization (Copyright (2002) American Chemical Society. Reprinted from Ref. [14] with permission).

Name	Functions
Collagen	Structural protein found in many tissues
Bone sialoprotein (BSP)	Acid protein with poly(glutamic acid) run and RGD binds calcium
Osteonectin (ON) and osteopontin (OP)	Glycoproteins that may either nucleate or block HA mineralization
Chondroitin sulfate (ChS) and keratan sulfate	Large molecular weight, sulfated glycosaminoglycans that are found in cartilage and bone tissues
Osteocalcin (OC)	Inhibits bone formation; does not appear to affect HA mineralization
Biglycan and decorin	Proteoglycans that bind to type I collagen and are involved in assembly of bone matrix
Thrombospondin and fibronectin	Matrix glycoproteins that bind to integrins and ECM components (collagen, fibrin, etc.)

Table 3

Common terms and their definitions [10,14,22,23].

Bioactive	A bioactive material is a material that can induce specific biological activity. In bone tissue engineering “a bioactive material is a material on which bone-like hydroxyapatite will form selectively after it is immersed in a serum-like solution” [22].
Biodegradation	It is a destructive process and involves transformation of a substance into new compounds through chemical (hydrolysis or oxidation) or biochemical reactions (enzymatic cleavage) or the actions of microorganisms such as bacteria [10].
Osteoconductivity	A property of a biomaterial that facilitates the formation of new bone structure. “Osteoconductive bioceramics allow attachment, proliferation, migration and phenotypic expression of bone cells leading to formation of new bone” [23].
Osteoblast	Osteoblasts are mononuclear cells originated from mesenchymal progenitor cells, responsible for production and mineralization of the bone matrix by regulating the local calcium and phosphate concentrations to promote apatite mineralization. Osteoblasts synthesize collagen and glycoproteins to form the bone matrix, and later they can become osteocytes.
Osteoclast	Multinucleated bone cells associated with the breakdown and resorption of osseous tissue through enzymatic action.
Osteoinductivity	The ability of the biomaterial to induce *de novo* bone formation [23]. Osteoinduction could be defined as the process of recruitment and stimulation of undifferentiated, pluripotent cells to form bone-forming cells, such as preosteoblasts, osteoblasts, and finally osteocytes [14].
Osteogenesis	The process of bone growth and regeneration. Includes osteoconduction and osteoinduction.
Angiogenesis	The process of developing new blood vessels. Newly formed blood vessels are involved in nutrient supply and transport of macromolecules during bone repair and regeneration.

Table 4

Properties of different calcium phosphates [10,11,24,33,34].

Calcium phosphates	Abbreviations	Chemical formula	Mineral name	Ca/P molar ratio	Solubility product
Monocalcium phosphate monohydrate	MCPM	$Ca(H_2PO_4)_2.H_2O$	–	0.5	7.2×10^{-2}
Monocalcium phosphate	MCP	$Ca(H_2PO_4)_2$	–	0.5	7.2×10^{-2}
Dicalcium phosphate dihydrate	DCPD	$CaHPO_4.2H_2O$	Brushite	1.0	2.5×10^{-7}
Dicalcium phosphate	DCP	$CaHPO_4$	Monetite	1.0	1.26×10^{-7}
Octacalcium phosphate	OCP	$Ca_8H_2(PO_4)_6.5H_2O$	–	1.33	2.51×10^{-97}
α-Tricalcium phosphate	α-TCP	$\alpha\text{-}Ca_3(PO_4)_2$	–	1.5	3.16×10^{-26}
β-Tricalcium phosphate	β-TCP	$\beta\text{-}Ca_3(PO_4)_2$	Whitelockite	1.5	1.25×10^{-29}
Amorphous calcium phosphate	ACP	$Ca_3(PO_4)_2.nH_2O$	–	1.2–2.2	*a*
Calcium-deficient hydroxyapatite	CDHA	$Ca_{10-x}(HPO_4)_x(PO_4)_{6-x}(OH)_{2-x}\ (0 < x < 1)$	–	1.5–1.67	*b*
Carbonated apatite	CA	$Ca_5(PO_4,CO_3)_3$	Dahlite	1.67	–
Hydroxyapatite	HA	$Ca_{10}(PO_4)_6(OH)_2$	–	1.67	2.35×10^{-59}
Oxyapatite	OXA	$Ca_{10}(PO_4)_6O$	–	1.67	
Tetracalcium phosphate	TTCP	$Ca_4O(PO_4)_2$	Hilgenstockite	2.0	1×10^{-38}–1×10^{-44}

[a] Solubility product varies due to its metastable nature.

[b] Solubility product varies depending on the stoichiometry.

Table 5

The ion concentration comparison between SBF and blood plasma (Copyright (2002) Elsevier. Reprinted from Ref. [107] with permission).

Ion	Ino concentration (mM)	
	Blood plasma	SBF
Na^+	142.0	142.0
K^+	5.0	5.0
Mg^{2+}	1.5	1.5
Ca^{2+}	2.5	2.5
Cl^3	103.0	147.8
HCO_3^-	27.0	4.2
HPO_4^{2-}	1.0	1.0
SO_4^{2-}	0.5	0.5
pH	7.2–7.4	7.4

Table 6

Commonly used growth factors in tissue engineering for drug delivery applications [134–136].

Growth factor	Abbreviation	Functions
Bone morphogenic protein	BMP	BMPs are osteoinductive. Induces bone formation by causing the migration of mesenchymal stem cells and their differentiation into osteoblast. BMPs do not initiate osteoclast activity.
Transforming growth factor-β	TGF-β	Causes proliferation and differentiation of bone by stimulating migration of osteoprogenitor cells, and regulating cell proliferation, cell differentiation and extra cellular matrix (ECM) synthesis. Inhibits proliferation and differentiation of osteoclast progenitor cells.
Fibroblast growth factor	FGF	Induces angiogenesis by increasing osteoblast proliferation, and also a potent stimulant for wound healing
Insulin-like growth factor	IGF	Stimulates osteoblast proliferation and bone matrix synthesis. IGFs also stimulate osteoclasts.
Vascular endothelial growth factor	VEGF	Induces angiogenesis during and permeabilization of capillaries bone formation. Regulates migration, proliferation and survival of endothelial cells by nutrient supply through the newly formed blood vessels.
Platelet-derived growth factor	PDGF	A key regulator of wound healing/tissue repair. Stimulates bone cell proliferation and angiogenesis.
Epidermal growth factor	EGF	Participates in wound healing process by regulating keratinocyte phenotype
Placental growth factor	PGF	PGF, a member of VEGF family, stimulates angiogenesis.

Table 7

Some common drugs used in musculoskeletal disorders treatment.

Name	Type
Gentamicin [109,185,188,196,210]	Antibiotic
Vancomycin [102,109,194,213]	
Tetracycline [157,195]	
Alendronate [92,117,189,214]	A member of bisphosphonate drug, used to treat bone diseases like osteoporosis
Zoledronate [116]	
Human lactoferrin (hLFI-II) [187,188]	Antimicrobial peptide (AMP)
Cephalexin [186,191]	Semisynthetic cephalosporin antibacterial agent
Methotrexate [103]	Anticancer agent
Cis-Platin [46,190]	
Ceramide [75]	
Doxycycline hyclate (DOXY-h) [193]	Antibiotic, commonly used in dentistry to defeat periodontal pathogens
Ibuprofen [212]	A non-steroidal anti-inflammatory drug